SHORT-TERM AIR-SEA INTERACTIONS AND SURFACE EFFECTS IN THE BAFFIN BAY - DAVIS STRAIT REGION FROM SATELLITE OBSERVATIONS

J. D. Jacobs, R. G. Barry

B. Stankov and J. Williams

FINAL REPORT

to the

OFFICE OF POLAR PROGRAMS

NATIONAL SCIENCE FOUNDATION

NSF GV-28220

1972

Occasional Paper No. 4

INSTITUTE OF ARCTIC AND ALPINE RESEARCH . UNIVERSITY OF COLORADO

SHORT-TERM AIR-SEA INTERACTIONS AND SURFACE EFFECTS IN THE BAFFIN BAY-DAVIS STRAIT REGION FROM SATELLITE OBSERVATIONS

J.D. Jacobs, R.G. Barry

B. Stankov and J. Williams

Final Report to

Office of Polar Programs

National Science Foundation

NSF GV 28220

October, 1972

ABSTRACT

A study of meteorological satellite data was undertaken for purposes of calculating surface energy budgets in relation to synoptic-term events in the Baffin Bay - Davis Strait region. Visual and infrared imagery, infrared temperature maps, satellite derived atmospheric temperature and humidity profiles, and conventional synoptic data were used to determine exchange rates for selected days in June, July, and August, 1970. An evaluation was made of presently available satellite data in comparison with surface and airborne measurements in the region. While problems remain in the satellite data interpretation and in the simplified energy budget model used, it is demonstrated that assessments of short-term (daily) variations in surface fluxes are possible using this approach. Continuing field investigations and improved satellite coverage will permit an extension of this work in developing a synoptic energy budget climatology for this important sector of the Arctic.

1. THE REGIONAL ENERGY BUDGET PROBLEM

1.1 Introduction

Difficulties in assessing interactions between the atmosphere and ocean, particularly in arctic regions, derive in part from incomplete knowledge of exchange parameters. Intensive measurements in the field can provide a better understanding of the processes involved, but any attempt to apply these results routinely on a large areal scale is likely to be frustrated by the shortage of data. Meteorological satellites are beginning to fill gaps in coverage, not only in terms of conventional meteorological observations, but also with regard to the radiation budget.

Recognition of the importance of synoptic-scale interactions to interannual variations in glacial mass balance and sea ice conditions in the eastern Baffin Island region prompted an investigation of the applicability of satellite data to energy budget calculations in this data-sparse region. The synoptic energy budget approach to problems of climatic variability in the Arctic has been developed along general lines by Vowinckel and Orwig (1969). By combining field measurements with a variety of satellite and synoptic data, we have tried to produce the framework of a synoptic energy budget climatology usable in modeling climatic variations for a particular polar region.

Our previous work indicates that the summer months are the most critical in determining interannual variations and probably also secular trends in glacial and sea ice conditions (Andrews, et al., 1972, Jacobs and Barry, 1972). Hence, the satellite data study

described here was confined to portions of the summer months of 1970 and 1971, periods which coincided with our various field programs in the area of eastern Baffin Island and the adjacent Davis Strait (Figure 1.1). It is in this region that ground truth was obtained. The scale of available satellite data also permitted a larger region to be considered, between 50° to 80° W and 60° to 75°N, though with greater uncertainty.

1.2 Synoptic Energy Budget Calculations

The basic idea underlying the synoptic energy budget approach is that for a particular location, time of year, and type of regional circulation pattern, there exists a characteristic regime of heat, moisture, and momentum exchange between the surface and the atmosphere. By studying interactions associated with individual synoptic systems (events), as well as the frequencies of such systems, a synoptic energy budget climatology may be constructed for that region.

Considering only the radiative and turbulent heat terms, the surface energy budget is given by

$$R_n = LE + H + G \qquad (1)$$

where R_n is net radiation, LE and H the latent and sensible heat fluxes, respectively, and G is the net heat flux to the substratum which may include heat of fusion or sublimation in the case of snow and ice. Net radiation is the sum of the incident and reflected short wave terms S and $S(1-\alpha)$, where α is the surface albedo, and the atmospheric and terrestrial long wave fluxes $L\downarrow$ and $L\uparrow$. Thus

$$R_n = S(1-\alpha) + L\downarrow - L\uparrow \qquad (2)$$

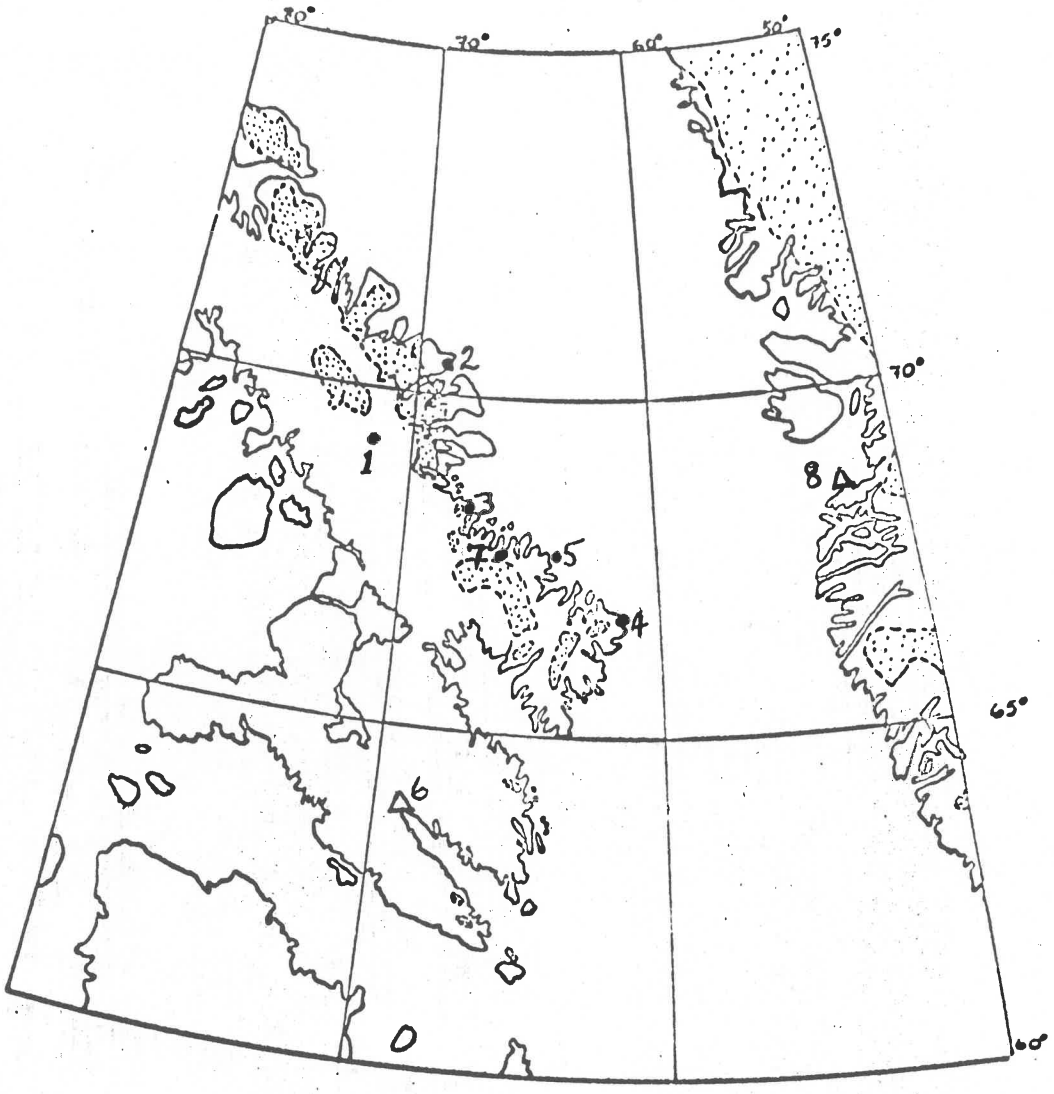

1. Dewar Lakes
2. Clyde
3. Cape Hooper
4. Cape Dyer
5. Broughton Island
6. Frobisher
7. Boas Glacier
8. Egedesminde

Figure 1.1

Location of existing surface (.) and upper air (Δ) observing stations in the Baffin study region.

The turbulent flux terms LE and H may be expressed in a variety of forms as functions of windspeed and vapor and temperature gradients.

For the purposes of the present study it is the ground flux term G which is of principal interest; that is, the heat flux to snow, ice, and water surfaces under a variety of synoptic conditions.

1.3 The Application of Satellite Data to Energy Budget Calculations

Clear sky insolation can be accurately calculated given solar declination and an average transmissivity for the region. That portion of the solar flux actually absorbed at the surface is determined by cloud conditions and surface albedo. Information on cloud cover and surface type is provided by a combination of visual and infrared satellite imagery. The results of field measurements of albedo of different surfaces and cloud effects are then applied in calculating the absorbed solar flux for a given situation.

The terrestrial long wave flux is obtained from satellite IR temperature maps using the Stefan-Boltzmann relationship, $L\uparrow = \varepsilon\sigma T^4$. An emissivity ($\varepsilon$) of unity can be assumed for snow, ice, and water since actual values are in the range 0.92-0.99 (Sellers, 1965). A finite difference form of the radiative transfer equation is used for the atmospheric flux term $L\downarrow$, where temperature and vapor profiles are obtained from satellite soundings (SIRS) in conjunction with radiosonde data. Satellite-derived temperature profiles and surface temperatures may also be used to assist in calculating the turbulent terms of the energy budget.

It is clear that the present generation of meteorological

satellites is capable of providing basic information for energy budget calculations in any region on a twice-daily basis. Realization of this potential requires the development of interpretative and analytical techniques in relation to data limitations and deficiencies and to the regional situation. This report is concerned with the examination of specific cases in this context.

2. REGIONAL ENERGY BUDGET STUDIES

2.1 Introduction

An attempt was made to obtain energy budgets near local noon on a daily basis for the months June, July and August of 1970 over a region which includes most of Baffin Island, Davis Strait, and Baffin Bay to 75°N (Figure 1-1). Satellite data used in this aspect of the study included ESSA-9 AVCS and APT pictures, minimum brightness composites, and Nimbus 4 THIR and SIRS (see Table 2.1).[1]

A preliminary study of these data by Reynolds (1971) produced regional budgets for five different synoptic types simplified from Barry's (1972) classification. The analysis showed realistic differences in exchange rates in accordance with cloud, airflow, and temperature characteristics of the various types. In that study AVCS and APT pictures were used to determine cloud and surface

---

[1] The satellite data and data products of interest in this study are listed in Table 1 together with selected references concerning their nature and applications. The reader is referred to these for a description of systems.

Table 2.1. Satellite data and data products considered in this study.

A. Visual Imagery and Products

Advanced Vidicon Camera System (AVCS) ESSA-8 & 9 (1)

Automatic Picture Transmission (APT) ESSA-8 & 9 (1)

Image Dissector Camera System (IDCS) Nimbus-4 (2)

Minimum Brightness Composites of AVCS Imagery (3)

B. IR Imagery and Products

11.5 μm Temperature - Humidity IR Radiometer (THIR) - Nimbus 4 (2,4)

1:5 M Temperature Maps from Nimbus 4 THIR (1)

11.5 μm Scanning Radiometer (SR) Imagery - ITOS - 1 (4)

1:4 M Temperature Maps from ITOS - 1 SR (4)

C. Temperature and Humidity Profiles

Satellite IR Spectrometer (SIRS-B) Temperature and Humidity profiles at mandatory levels - Nimbus 4. (2, 5)

References 1. Anderson, et. al, 1969

2. Sabatini, 1970

3. McClain and Baker, 1969

4. Barnes, Chang, and Willand, 1969, 1972 a, b

5. Smith, Woolf, and Jacob, 1970.

conditions and surface temperatures were obtained by direct comparison of THIR positive transparencies with their accompanying grey scales. While this work served to suggest the magnitude of synoptic variations, the comparative crudeness of analytical techniques precluded determination of absolute exchange rates. Nevertheless, this study represented an improvement over work based strictly upon conventional data in that 1) regional snow, ice, and cloud cover are fairly well mapped and 2) surface temperatures appear to be accurate within a few degrees in areas of little cloud cover, thus providing useful information on variations in heating among surface types.

2.2 Mapping of Infrared Data

In an attempt to obtain a more objective interpretation of the THIR imagery, a densitometric technique was developed. A rectangular grid with 2mm spacing was superimposed on the film and the optical density measured at each interval, as well as for the gray scale on that particular film. A computer program was written incorporating the satellite track coordinates and gray scale calibrations to provide "corrected" temperatures in terms of geographical coordinates. An example of the resulting surface flux maps is shown in Figure 2.1.

Limitations on densitometric determinations of temperatures from THIR film strips have been discussed in some detail by Barnes et al. (1969). In our case the uncertainties were of two kinds: a temperature error due to a lack of uniformity in the films and a positional error resulting both from errors in the subsatellite track location on the film and from the limitations in the computer coordinate transformation program so far developed by us. Temperature errors were

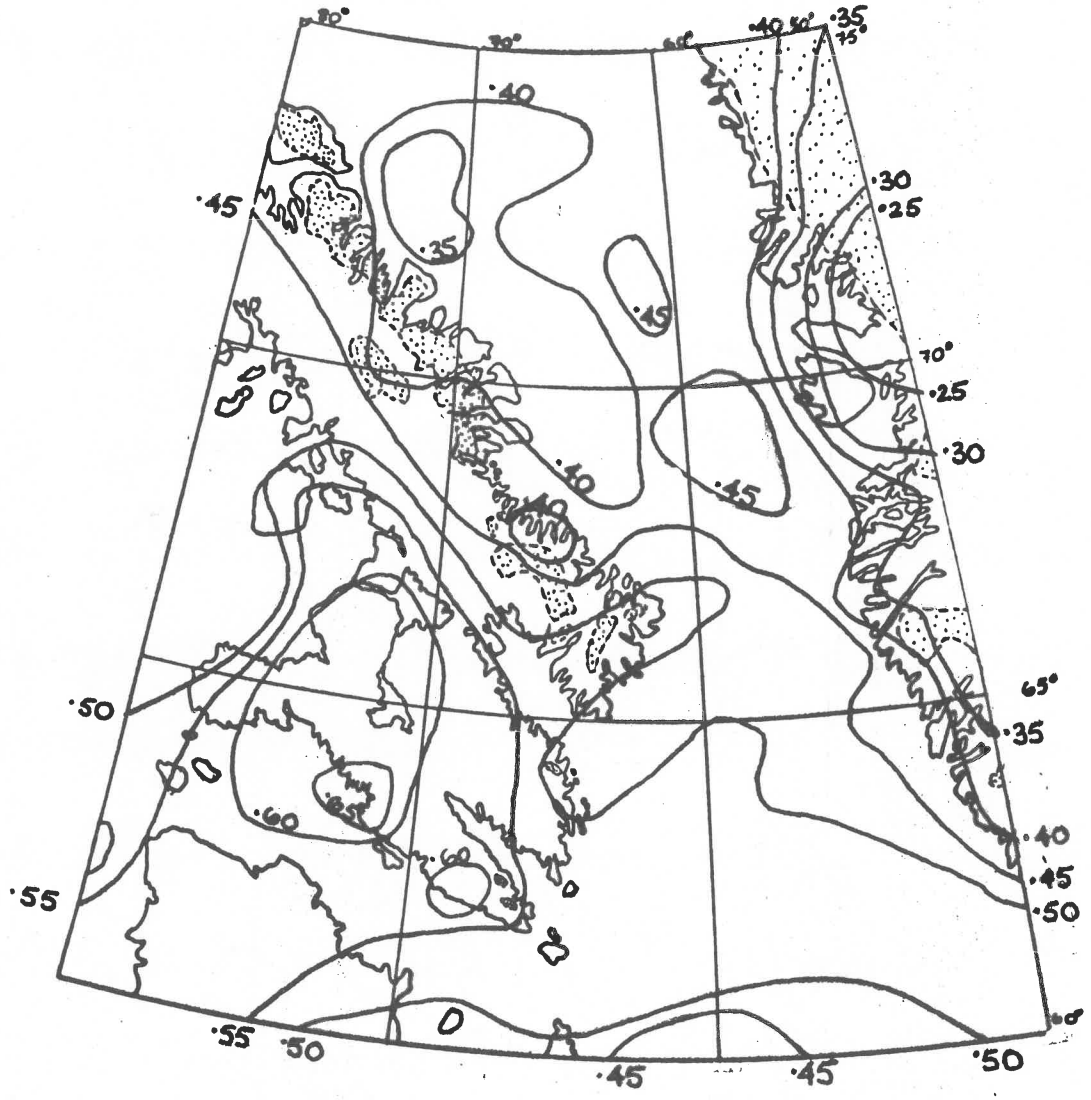

Figure 2.1

An example of a surface long-wave flux (σT^4) map derived from densitometric interpretation of NIMBUS 4 THIR, 26 July 1972.

always less than one gray scale step (15°K) near 273°K, as determined for snow and ice fields or open water. Positional inaccuracies were commonly as much as 2 degrees, although the temperature map could usually be displaced to conform to recognizable surface features.

Recognizing that the temperature errors in the THIR filmstrips arise mainly in photographic processing, a more direct approach to surface temperature mapping is to map equivalent temperatures directly from the radiometer signal record (Sabatini, 1970). Polar stereographic maps on a scale of 1:5 million were obtained from NASA Space Sciences Data Center for selected days during the 1970 summer. Because of their relatively large scale, such maps can be used effectively for mesoscale and local studies.

2.3 Mapping Cloud and Surface Features

The principal form of data used for mapping changing surface features, e.g. snow cover and sea ice, and for nephanalysis is satellite imagery in the visual range. The potential of good quality imagery is suggested by Figures 2.2 and 2.3. Interpretation of these pictures for the Baffin Island region is complicated by lack of contrasts between snow-covered land and mostly ice-covered sea and by frequent low cloud cover.

Compositing techniques have been used by McClain and Baker (1969) to assist in separating cloud from bright surface features. These minimum brightness composites rely on the transient character of clouds, which are thereby eliminated or at least reduced in the compositing process (Figure 2.4). Examination of 5-day minimum brightness

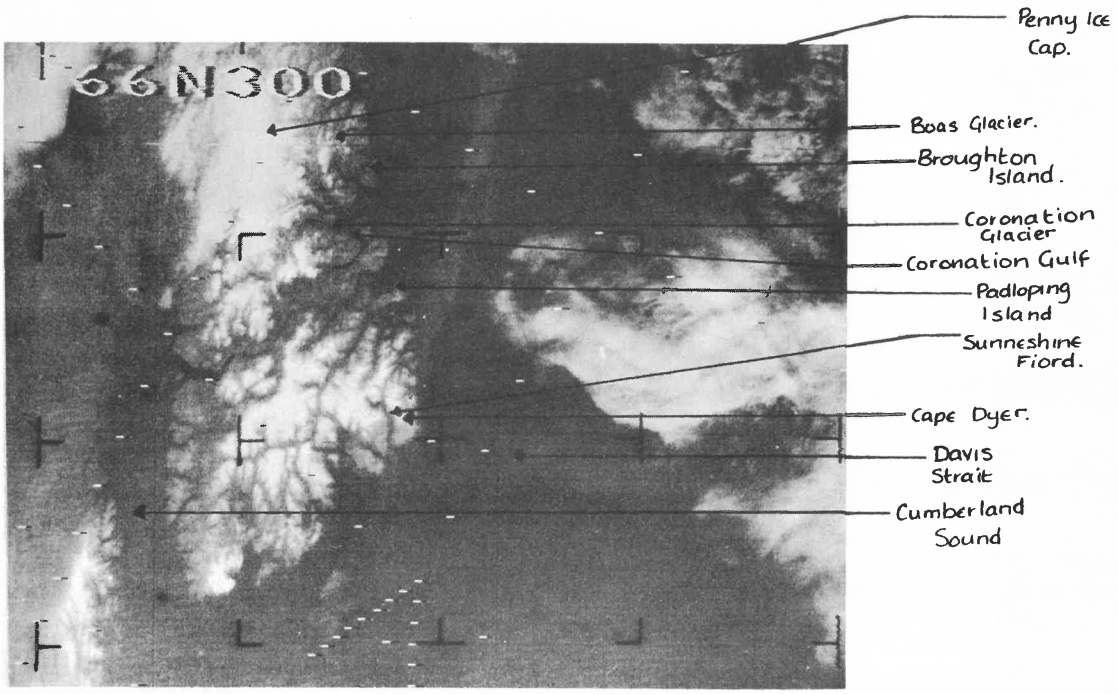

Figure 2.2

AVCS picture of the principal study area, Cumberland Peninsula and Davis Strait, from Nimbus I at an altitude of 530 km (4 September 1964). Autumn snowcover extends to sea level.

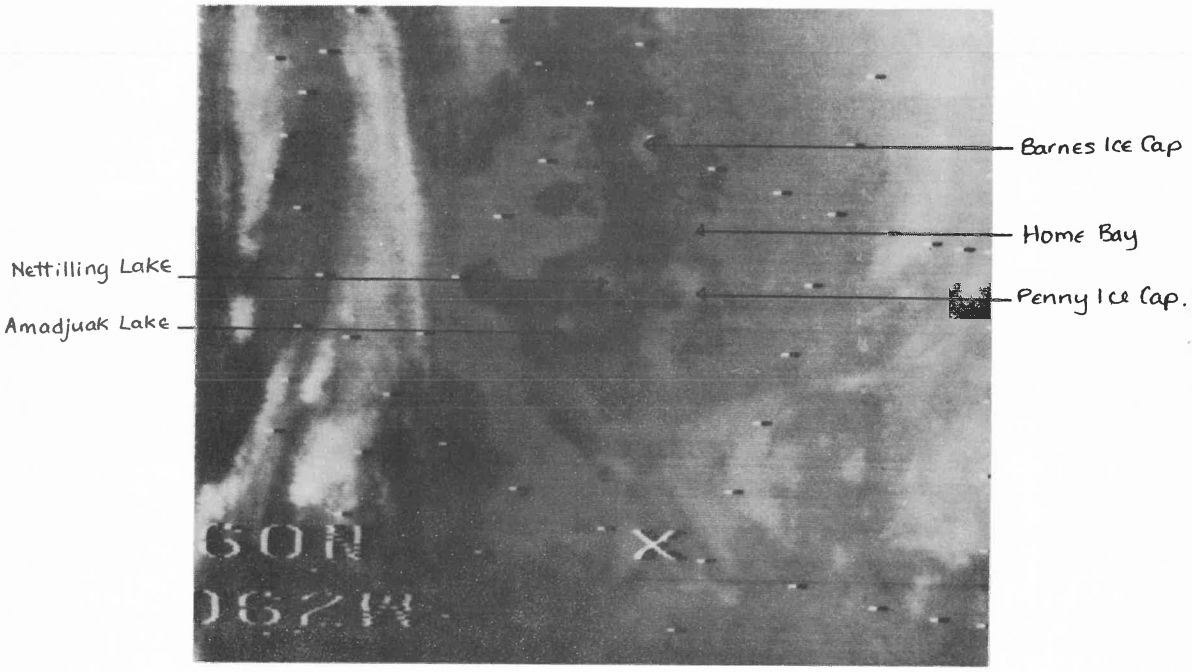

Figure 2.3

Nimbus 4 11.5μ THIR (10 Aug 1970) for Baffin Region showing contrasting temperatures among various surface features and clouds. Extensive ice and low stratus cloud in Home Bay are not visible due to their similar temperatures.

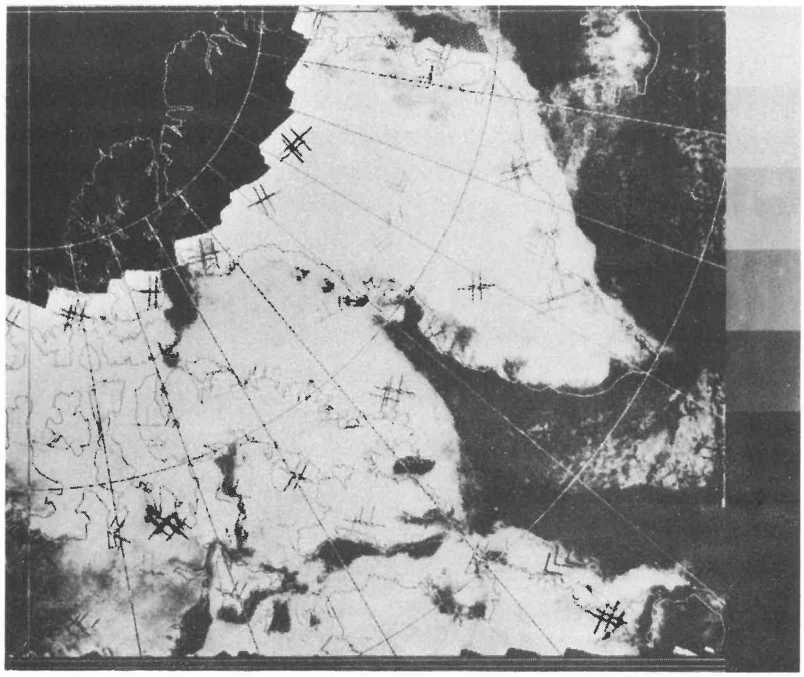

Figure 2.4

ESSA-9 AVCS Minimum Brightness Composite (8-12 June 1970) showing snow-covered land, sea-ice and persistent cloud.

composites for the summer of 1970 in conjunction with daily pictures showed the former to be of limited use in studies on a synoptic time scale. While large features such as the North Open Water and the pack margin could be located, details such as variations in pack density were smeared due to the presence of persistent cloud and to the movement of the pack itself.

For shorter-term mapping it was found preferable to examine the daily pictures directly. Several alternate forms were used. The most easily obtainable on a regular basis and in quantity[1] are the 35mm AVCS negatives (or prints made from these). These pictures were often found to be useless for our purposes due to the loss of resolution inherent in a 35mm format and generally poor quality of reproduction. Nimbus 4 IDCS prints and 70mm negatives, obtained for a portion of the period, were found to be of much better quality than the ESSA-9 AVCS. Some APT pictures from ESSA-8 and 9 were also used. These are 8 x 8 in. photofacsimile prints received directly from the satellite via an APT ground station. Having examined some of these pictures prepared in the Canadian Satellite Meteorological Laboratory, Downsview, Ontario, for sea-ice mapping purposes, i.e. with a special choice of contrast, we must conclude that a carefully prepared APT picture is preferable to the AVCS for our purposes. APT pictures were used with some success by Aber and Vowinckel (1972) in their study of the extent of the North Water.

---

[1]From National Weather Records Center, NOAA, Greenville, N.C.

Analysis of the visual imagery is direct and subjective. A recognizable surface feature is sought for purposes of orientation. If computer imposed grid lines and continental outlines are present, as with AVCS, these were used cautiously because of frequent positioning errors. The absence of cloud is immediately apparent in the fine detail of fiords, leads, and large floes. On the other hand, the masking of such surface features is indicative of cloud. An estimate of cloud (top) height is made by reference to the IR temperature map, which shows a cloudtop temperature where the surface is obscured. In the regional study discussed here, the amount of cloud (tenths) was estimated for each of 72 2.5 deg. (lat.) by 2.5 deg. (long.) grid spaces and this cloud was identified as low, middle, or high.

A more refined nephanalysis can be carried out along the lines suggested by Anderson and others (1969) in which satellite depicted cloud patterns are related to circulation features. Given sufficient information about typical cloud heights and thicknesses for the region in relation to synoptic types, recognition of a particular type permits one to infer values (within a certain range) of the essential parameters affecting the radiation and turbulent budgets.

Figures 2.5 (a-f) are examples of regional ice and cloud maps constructed using these techniques. As may be seen from the maps, fair agreement exists between estimated and reported cloud conditions in the vicinity of observing stations.

2.4 Temperature and Humidity Profiles for Atmospheric Flux Calculations

For the region of interest, there are presently only two radio-

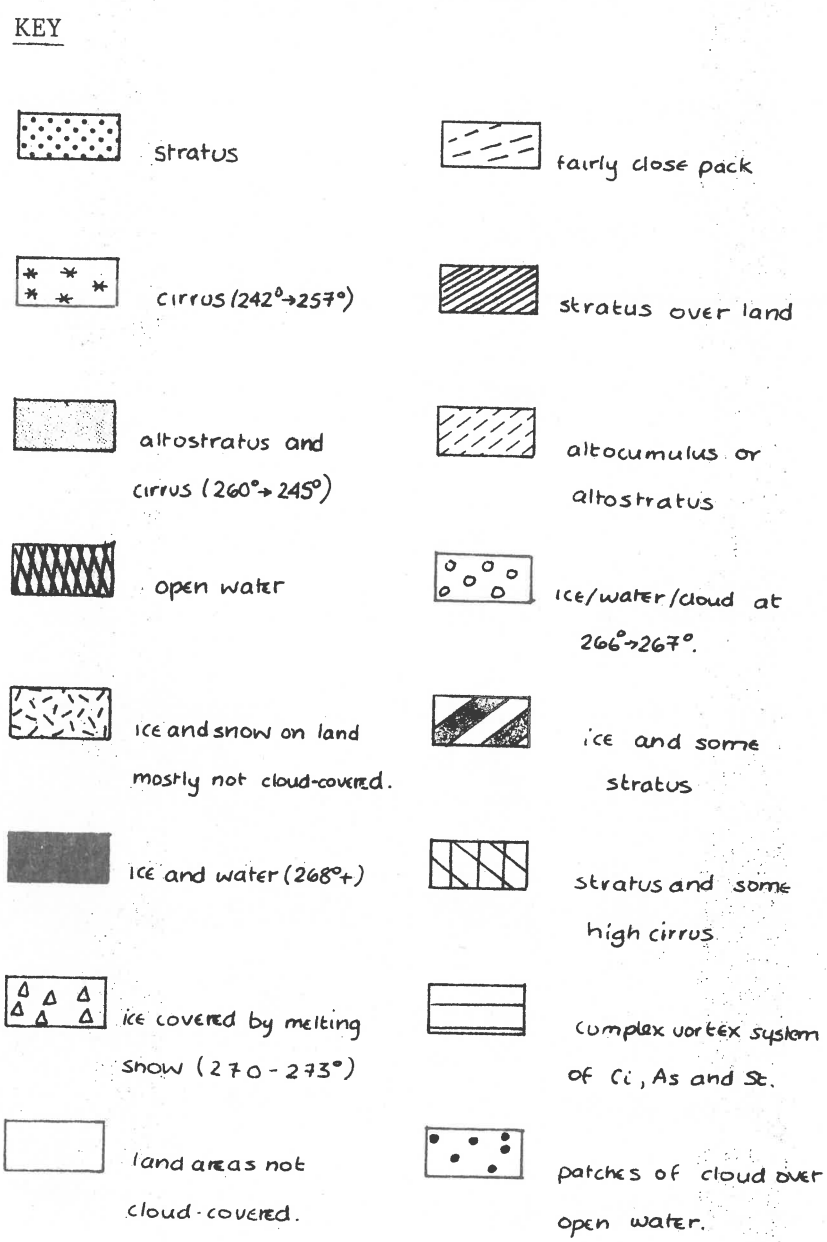

Figure 2.5 a-g

Regional maps of cloud condition (a-f) and ice cover (g) determined from satellite visual and infrared imagery. Cloud reports from surface stations are shown for comparison.

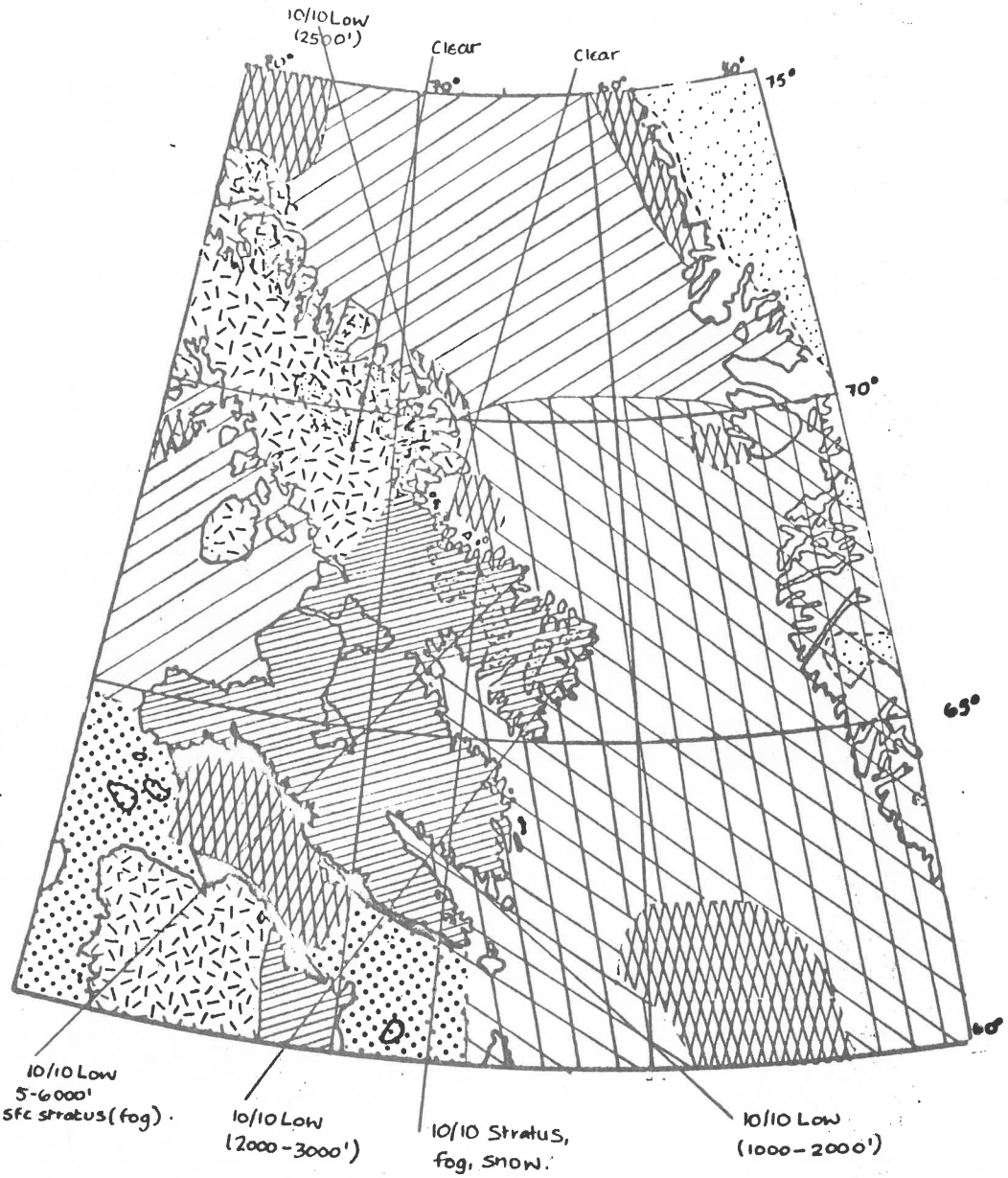

Figure 2.5a 26 June 1970

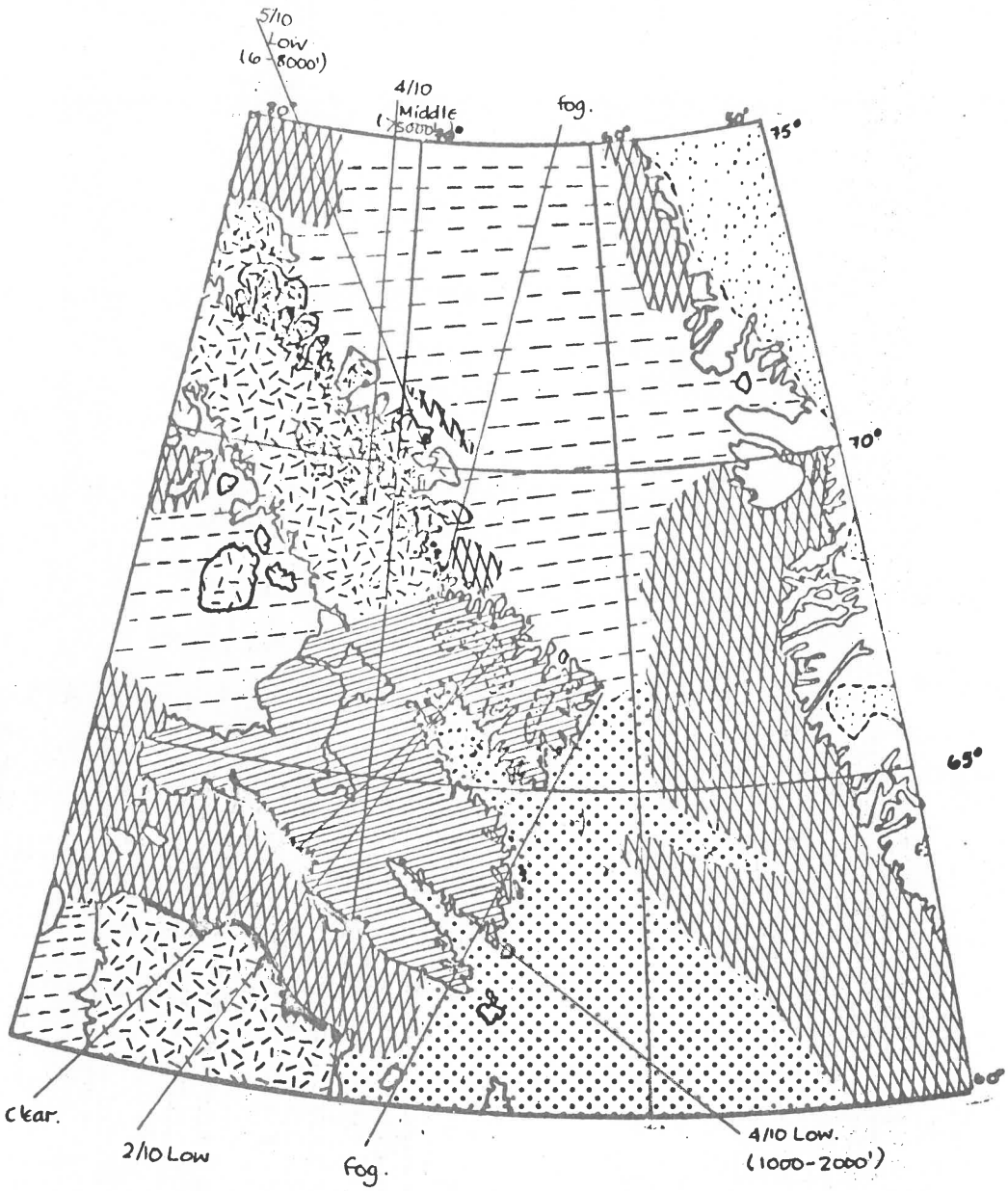

Figure 2.5b 28 June 1970

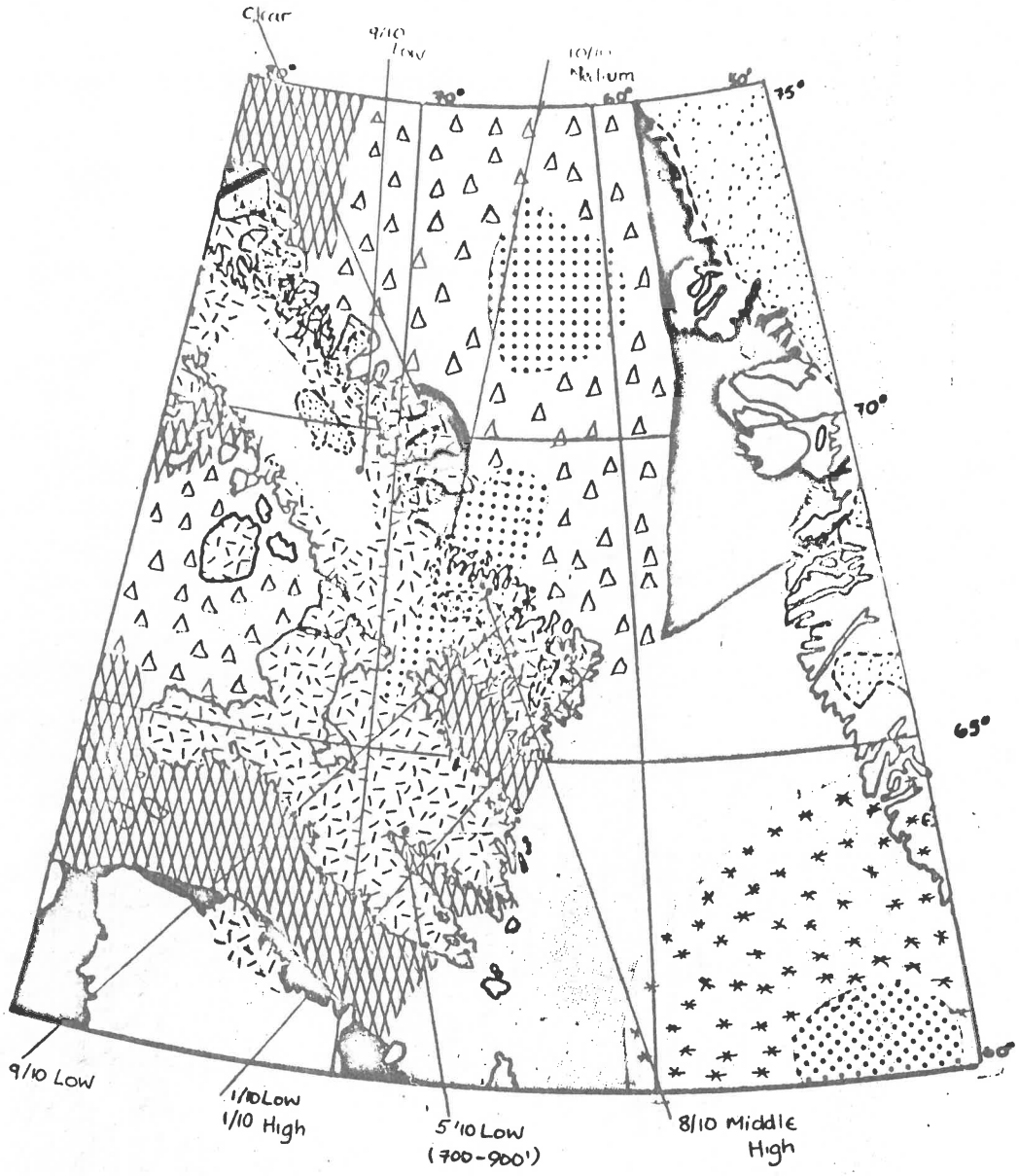

Figure 2.5c 2 July 1970

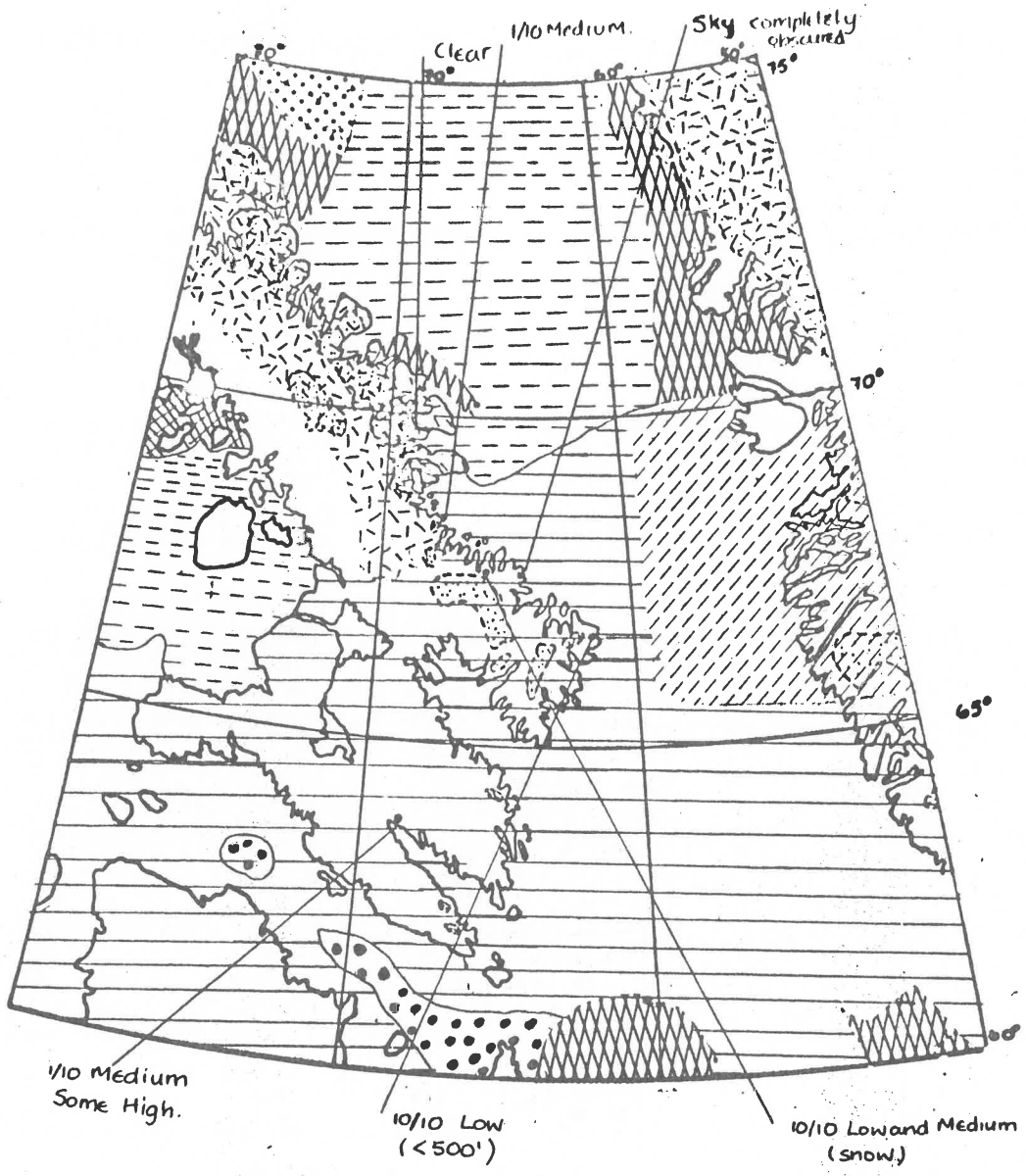

Figure 2.5d 8 July 1970

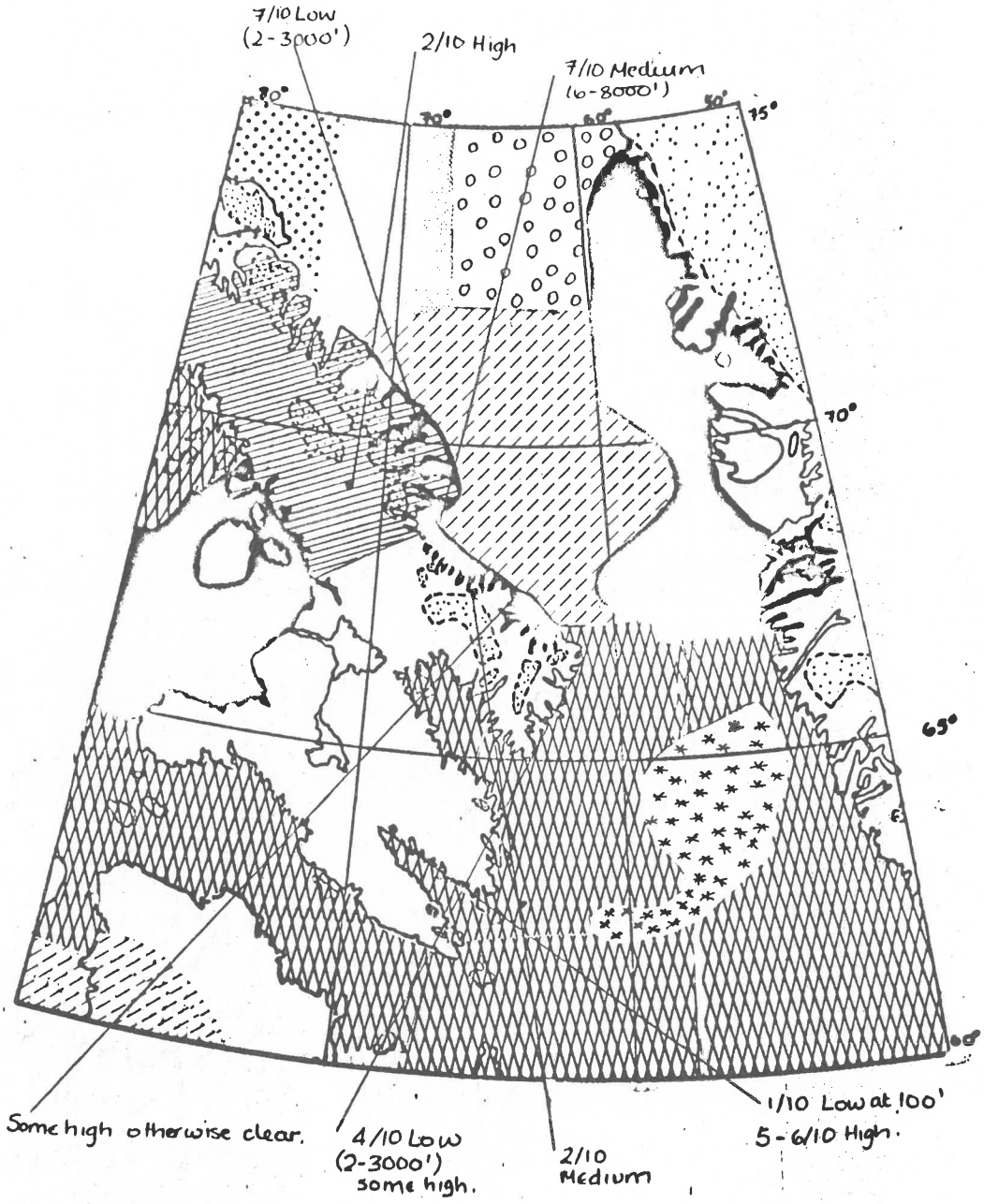

Figure 2.5e 26 July 1970

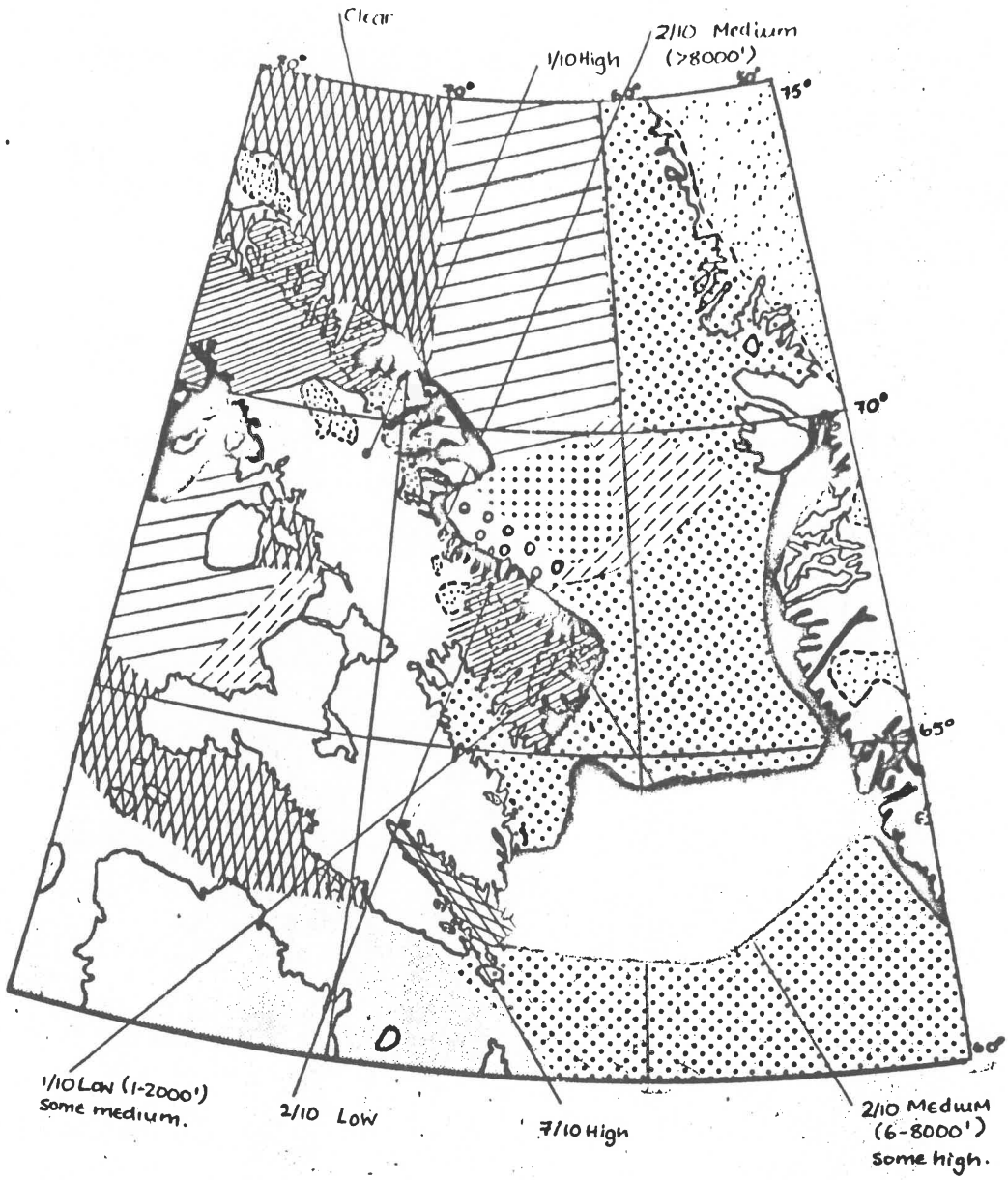

Figure 2.5f 27 July 1970

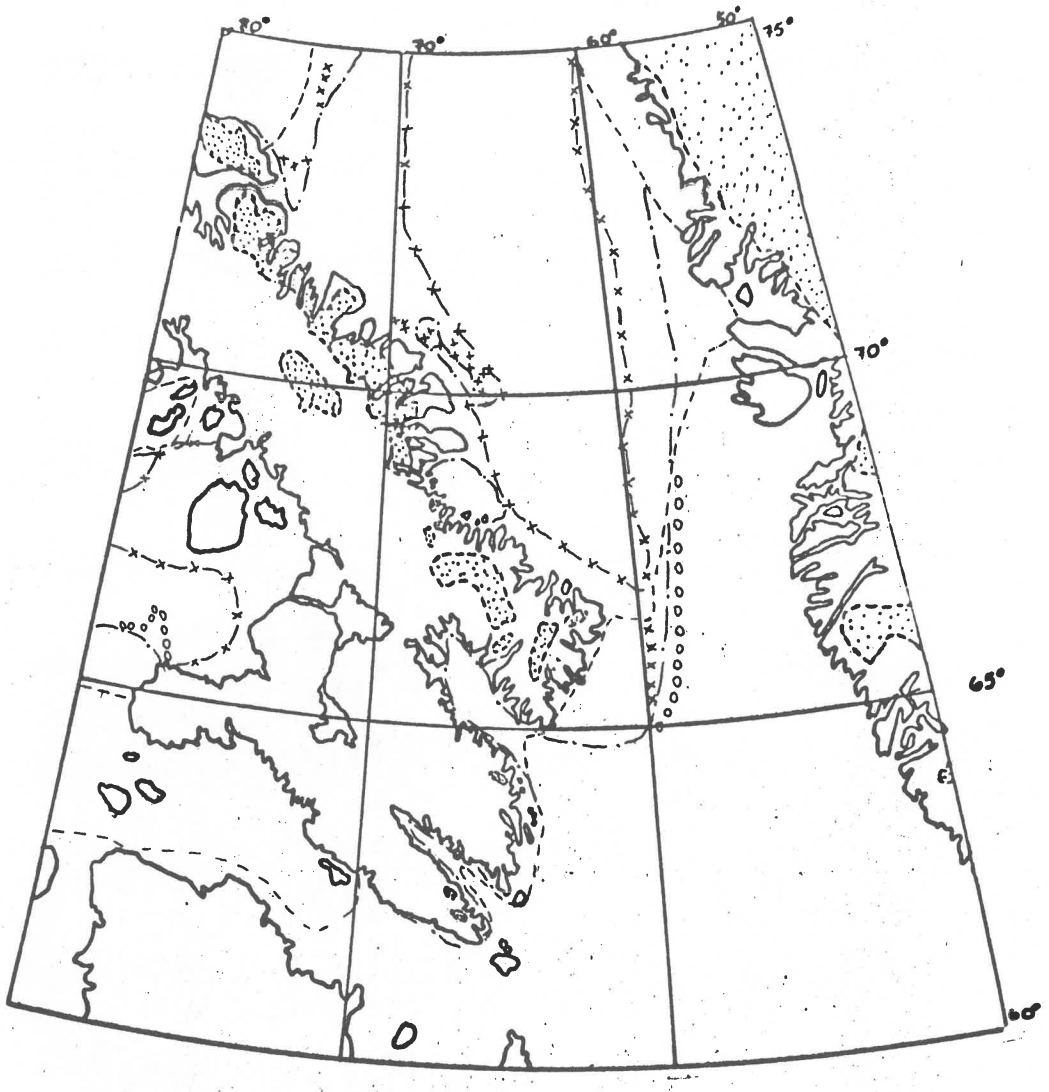

---- 26th June 1970

xxxxxx 28th June 1970

—.—.—. 1st July 1970

ooo'ooo 8th July 1970

—x—x—x 26th and 28th July 1970.

Figure 2.5g

sonde stations, Frobisher and Egedesminde (Fig. 1.1). A station at Clyde (70.5°N, 68.6°W) ideally located for our purposes, was closed at the end of July, 1970. In view of the great topographic diversity of the region, extrapolations from the two existing stations can provide only a very approximate representation of lower tropospheric conditions. Indications of the month-to-month variability of total vapor content over the area is shown by the maps for 1961-65 presented by Barry and Fogarasi (1968). The satellite infrared spectrometer (SIRS) promises to fill this data gap with an additional ten or more twice-daily soundings. For the summer 1970 period, profiles were available from the Nimbus 4 system, (SIRS-B), although not on a regular basis due to system malfunctions. Table 2.2 shows the relative density of coverage for the June-August, 1970 period.

Table 2.2 Density of SIRS soundings for Baffin Region June-August, 1970.

Number of Soundings within Region	Percent of Days June-August, 1970
0	28
1 - 5	32
6 - 10	36
10 - 14	4

Because not all of the spectrometer channels were usable, the quality of the data was below expectations; this affected moisture profiles in particular. Nevertheless, comparisons made with soundings at Clyde

and Frobisher showed generally close correspondence, confirming the applicability of SIRS data to the present study. Figures 2.6 a-e are examples of such comparisons for five days chosen for detailed analysis. SIRS values were requested for mandatory pressure levels. In view of the fact that the inversion near 900 mb fails to appear it would be highly desirable to obtain all levels in the future in order to improve the representation near the surface.

2.4 Regional Budget Calculations

The amount of solar radiation reaching the surface, Q, was determined using an empirical formula of Lumb (1964). For OWS Alfa (62°N, 33°W), he developed an expression

$$S\downarrow = 1.95fs \qquad (\text{cal cm}^{-2}\text{min}^{-1})$$

where 1.95 = solar constant

s = mean sine of solar altitude

$f = a + bs$ (where the constants a and b depend on cloud type and amount)

$$s = \sin a$$
$$= \sin \phi \sin \delta + \cos \phi \cos \delta \cos t$$

where ϕ = latitude

t = time angle of the sun (1.308 radians)

δ = declination

$$\delta \simeq -23.5\cos \left\{ \frac{2\pi}{365} (D + 9) \right\}$$

where D = day number.

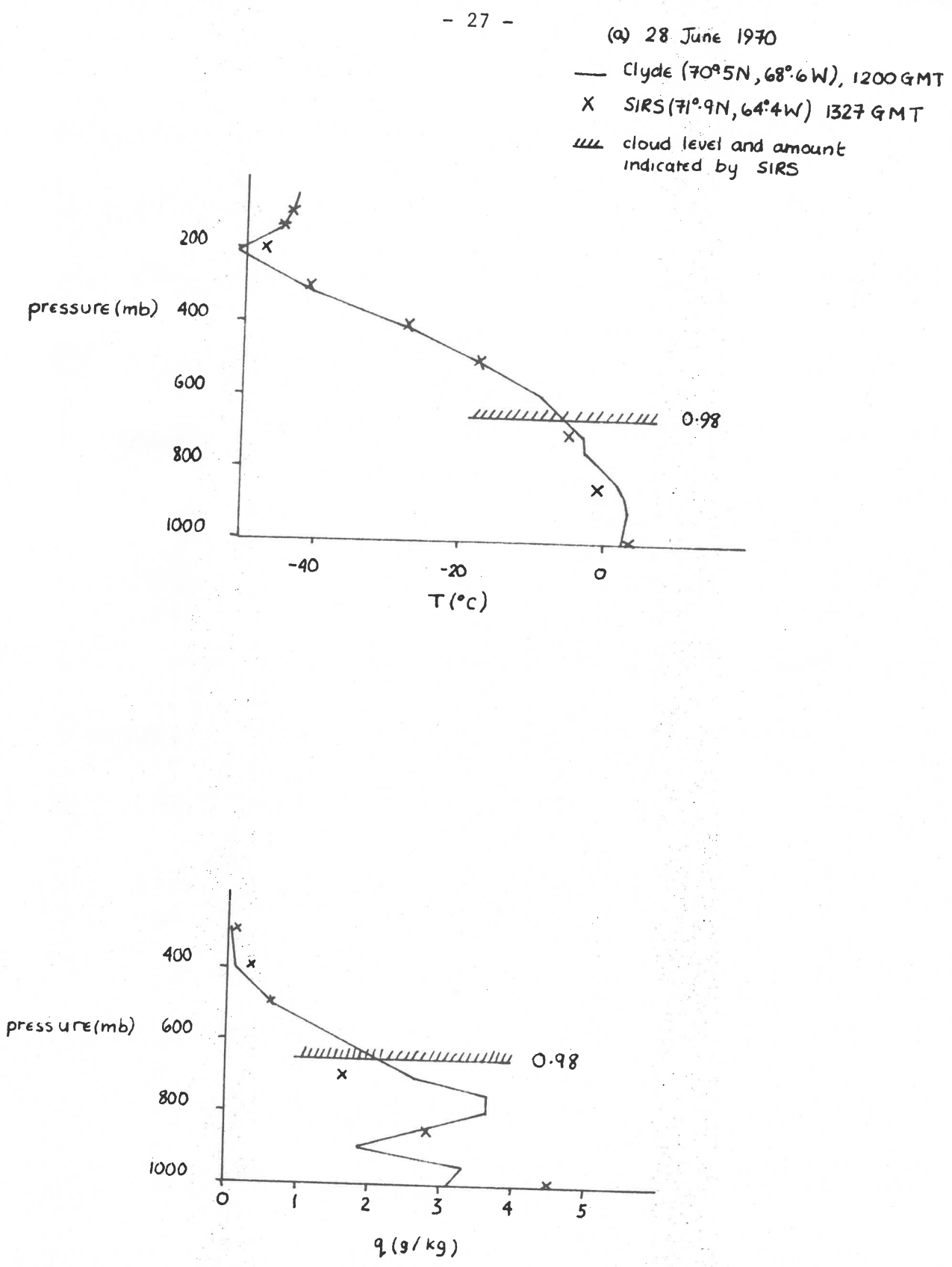

Figure 2.6 a-e Comparison of radiosonde and SIRS-B temperature and humidity profiles for selected days.

(b) 2 July 1970

Clyde 1200 Z

SIRS (71·8°N, 65·5°W) 0621 Z

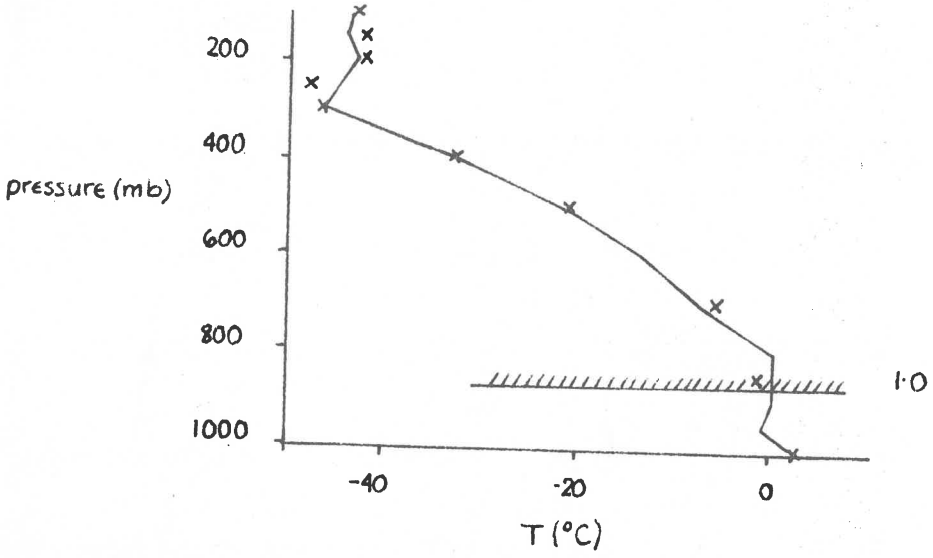

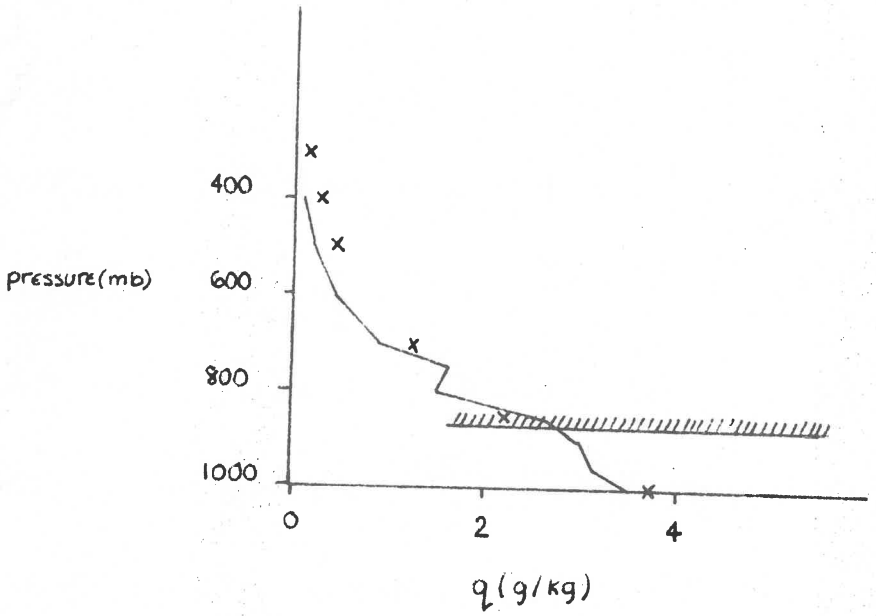

(c) 8 July 1970
Clyde 1200Z
SIRS (71·1N, 67·1W) 0621Z

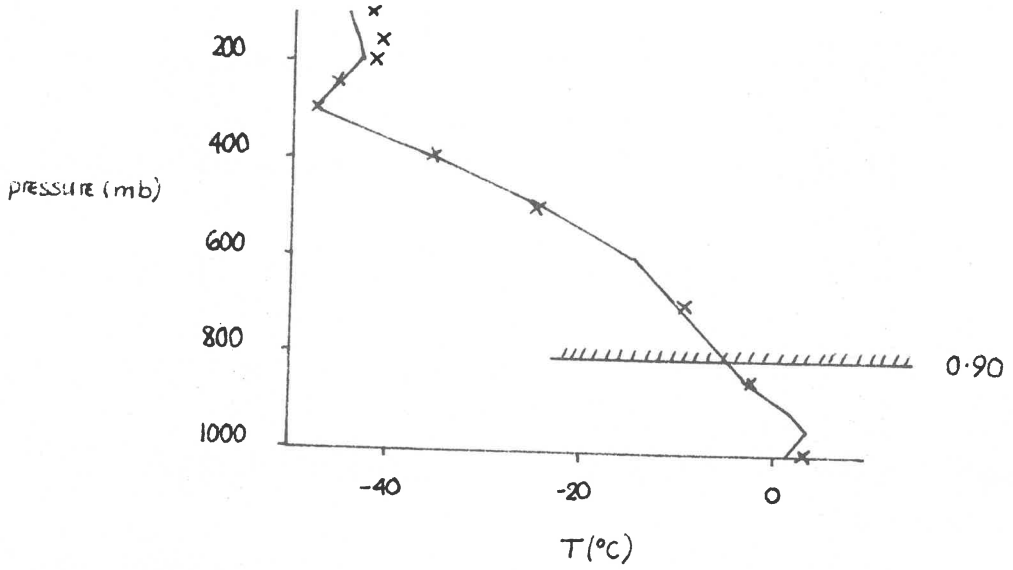

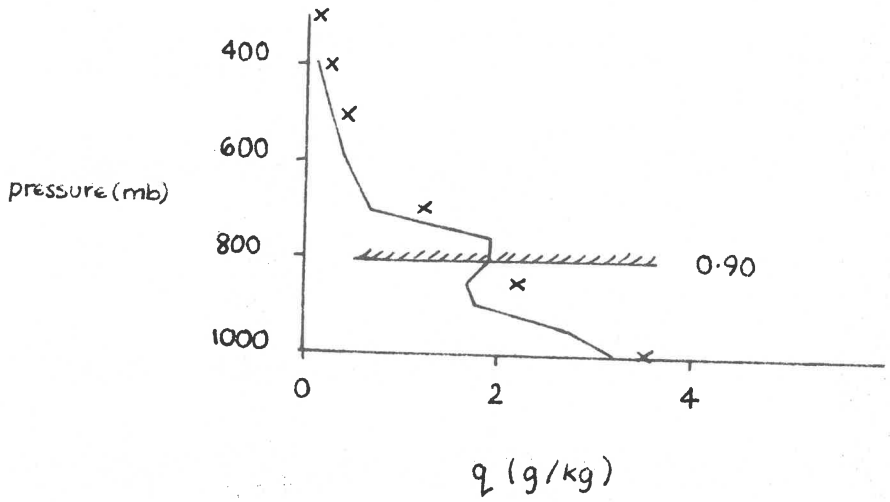

(d) 26 July 1970
Clyde 1200
SIRS (72·1°N, 72·8°W) 0652 GMT

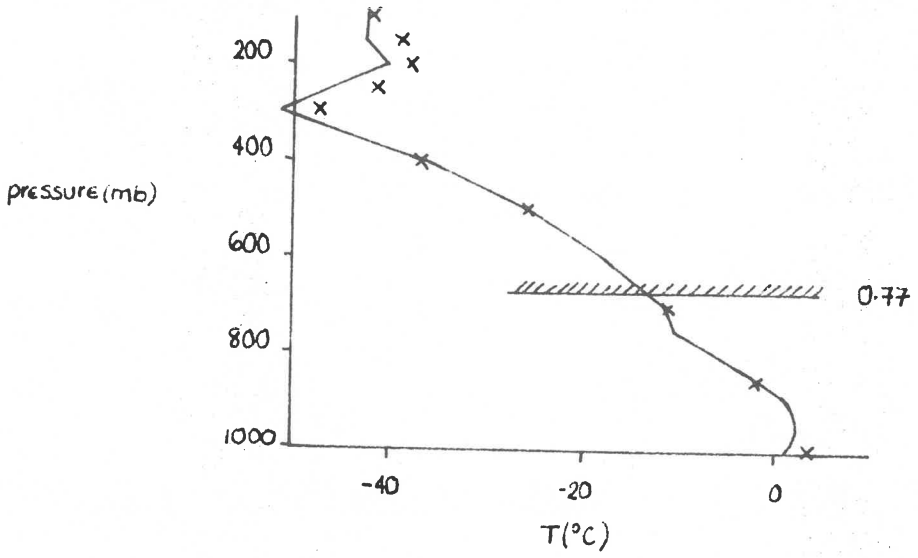

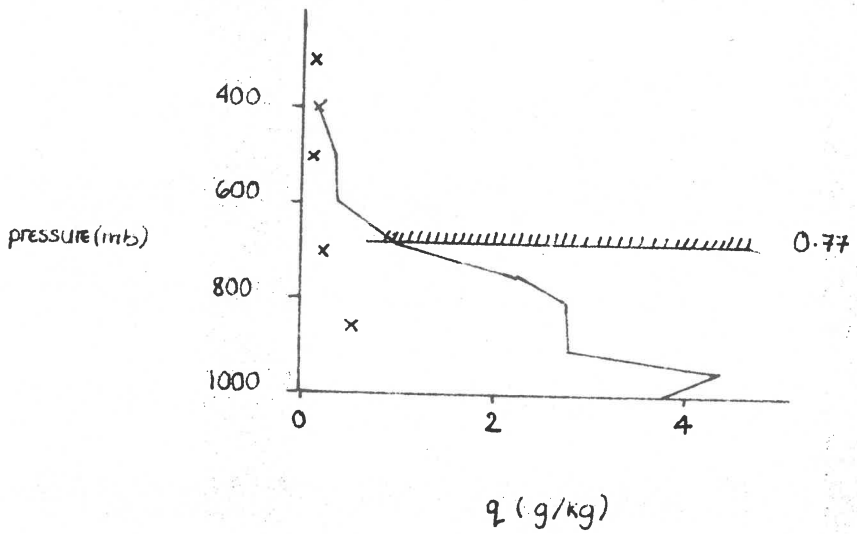

(e) 27 July 1970

Clyde (70·4°N, 68·6°W) 1200Z

SIRS (71·4°N, 71·3°W) 0752Z

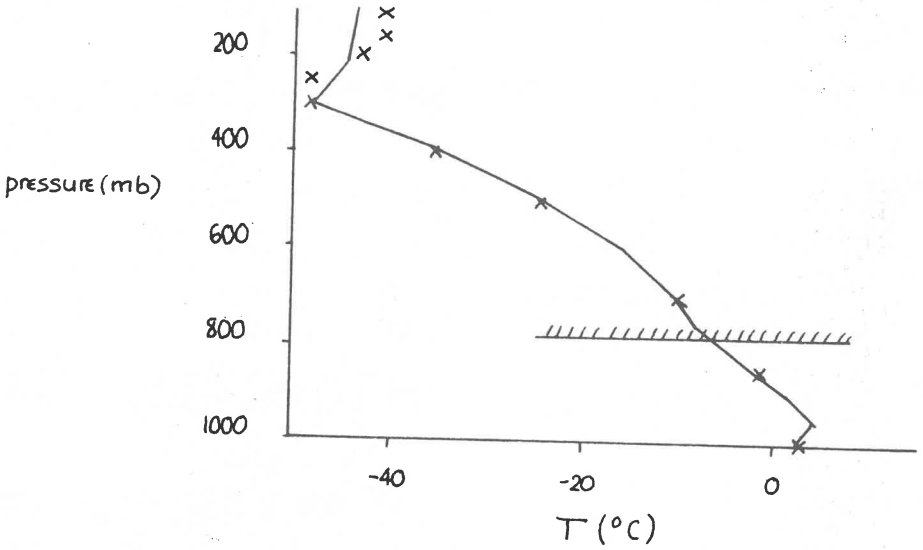

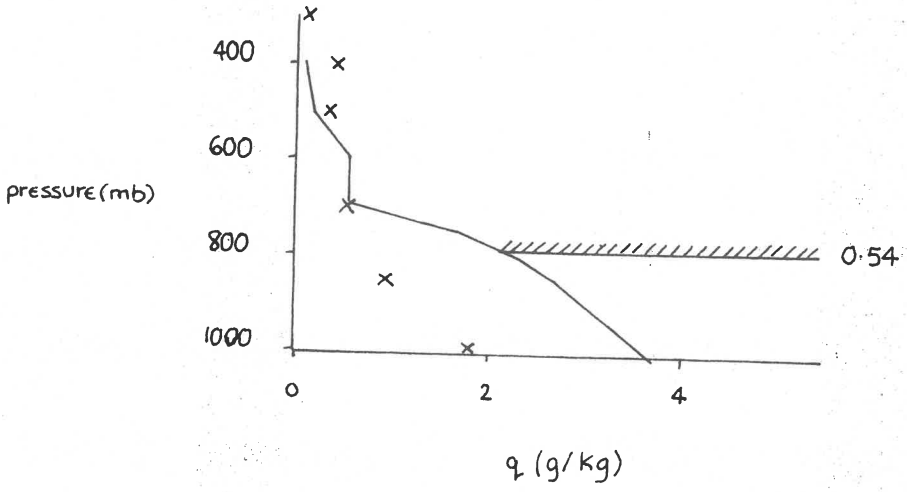

Following Lumb, f is determined by empirical regression equations. Six of Lumb's categories of cloud condition have been used in the present study (Table 2.3). Although derived from measurements made in the North Atlantic, these expressions are considered more appropriate to the present study than any of several more general forms. Solar radiation data now being obtained at the Broughton Island observing station will be used in an empirical model having more direct validity to the Davis Strait region.

The solar radiation absorbed at the surface (S_s) is obtained from

$$S_s = S\downarrow(1-\alpha)$$

where a is the surface albedo. The following albedos were assumed:

	Albedo
Snow	0.85
Ice (July)	0.65
Ice (August)	0.45
Water	0.08
Tundra	0.15

The calculations were carried by means of a computer program (SUNNY). Input data on ice distribution, cloud amount and type were obtained from the visual satellite imagery. The interpretation was plotted on a base map of the area and values representing 2.5° latitude-longitude areas were punched onto cards (Figure 2-7). Clouds were evaluated only in the three general categories low, medium and high, although even this may present difficulties with layer cloud.

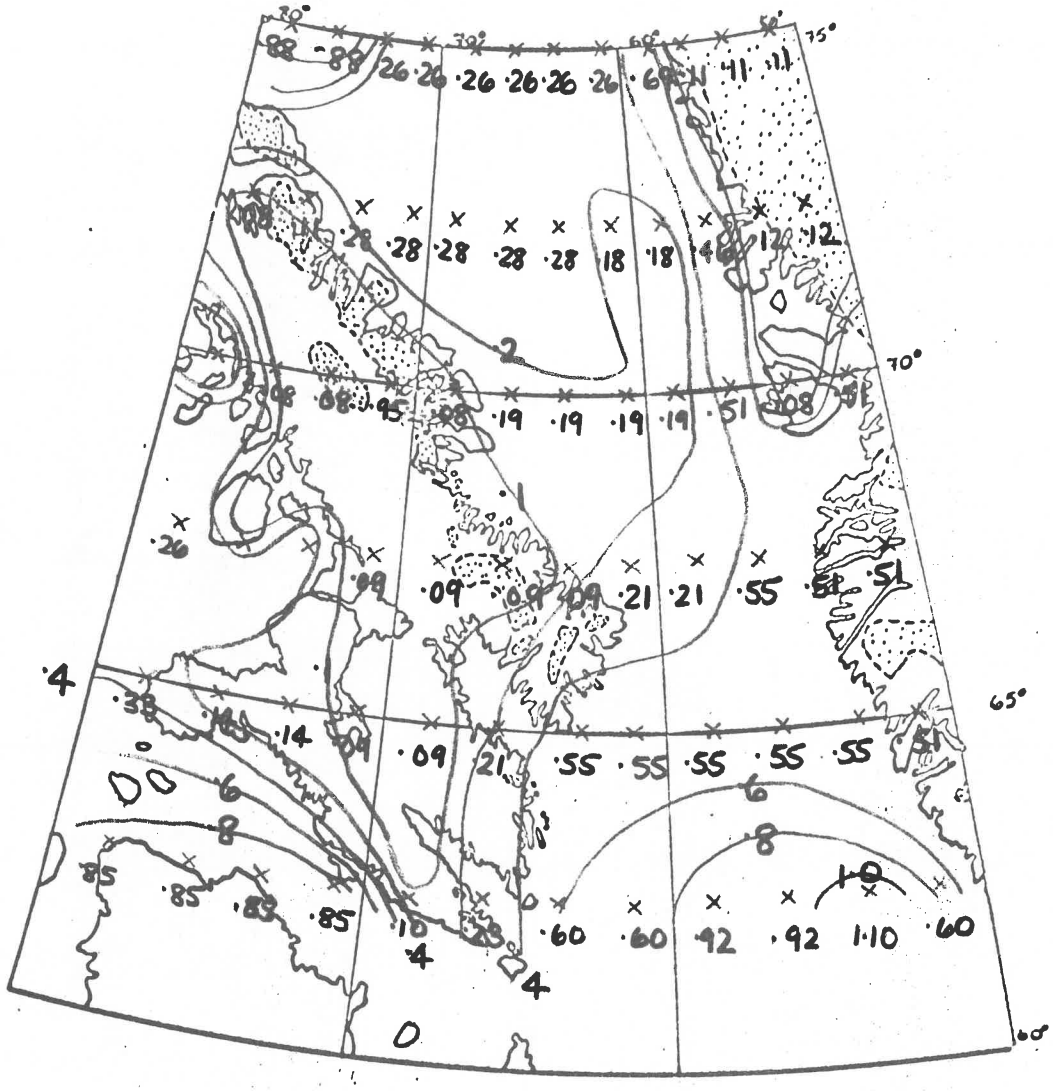

Figure 2.7a 26 June 1970

Figure 2.7 a-f

Solar radiation absorbed at surface midday (cal $cm^{-2} min^{-1}$) for selected dates.

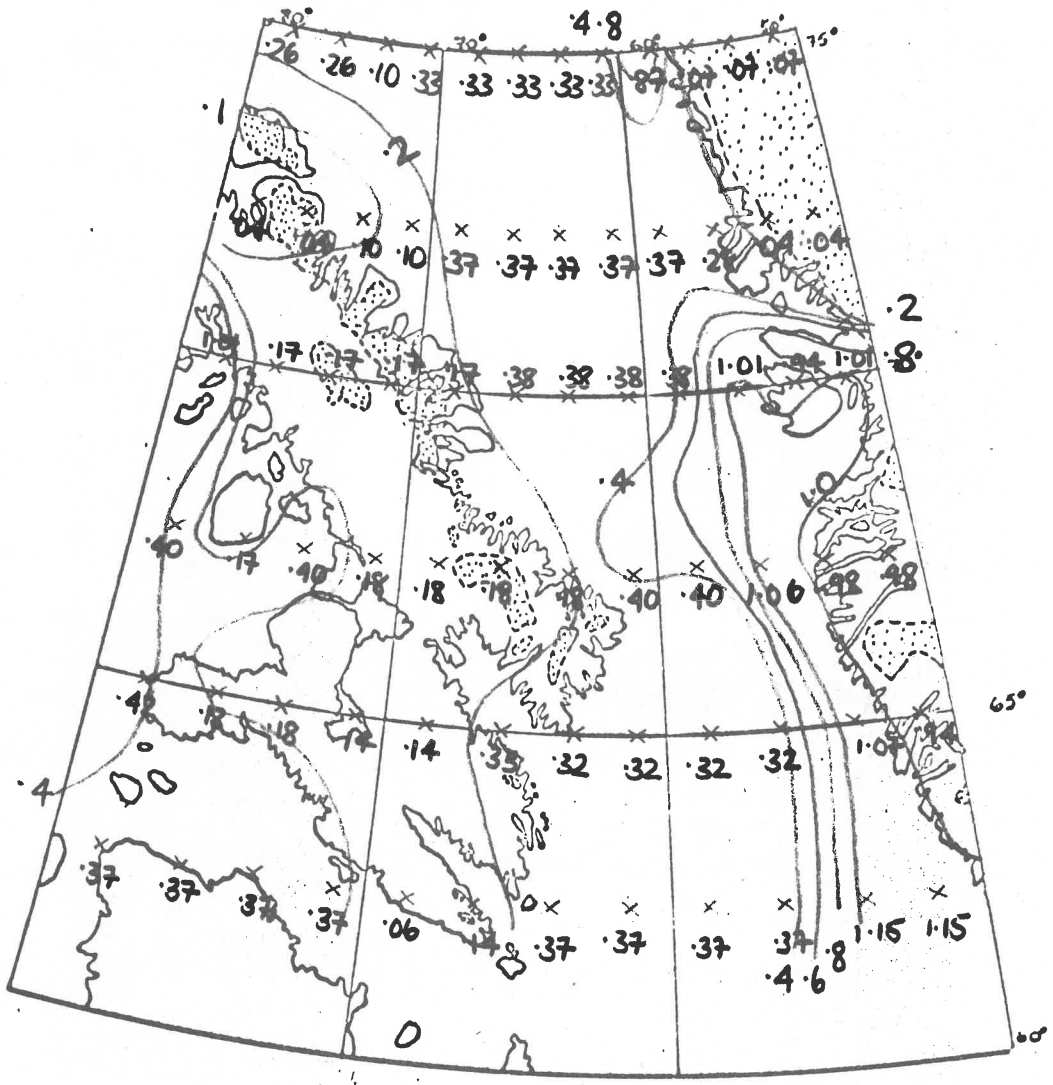

Figure 2.7b 28 June 1970

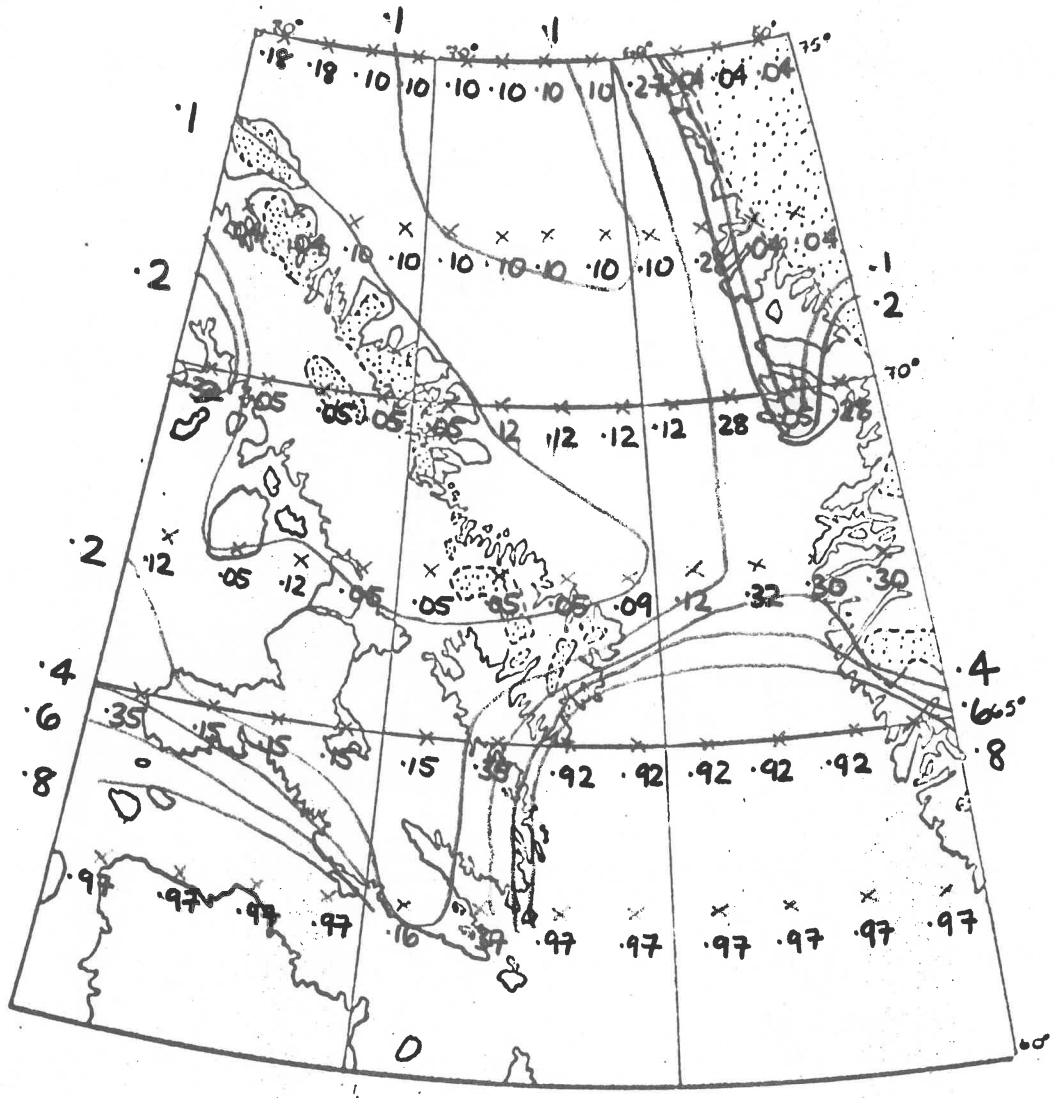

Figure 2.7c 2 July 1970

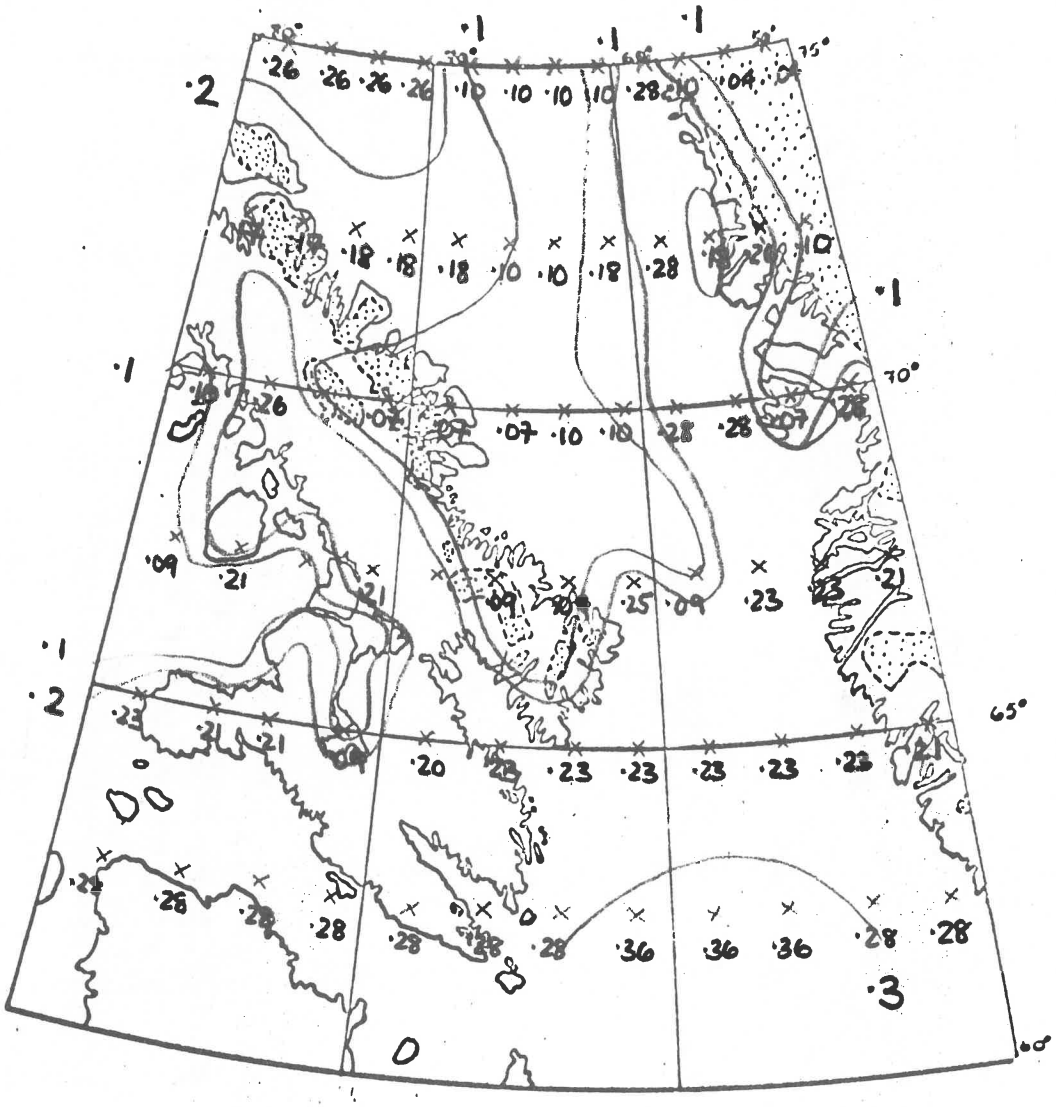

Figure 2.7d 8 July 1970

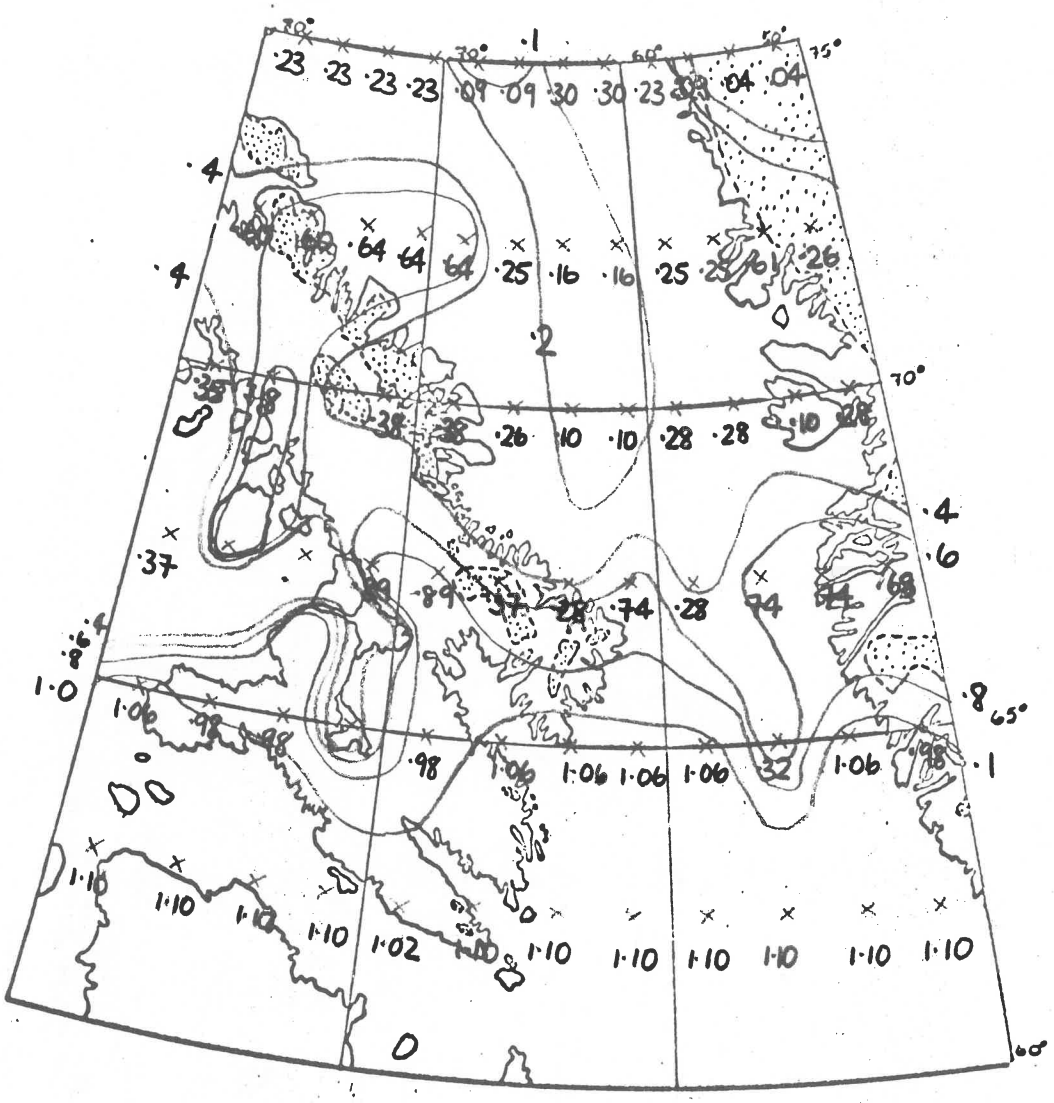

Figure 2.7e

26 July 1970

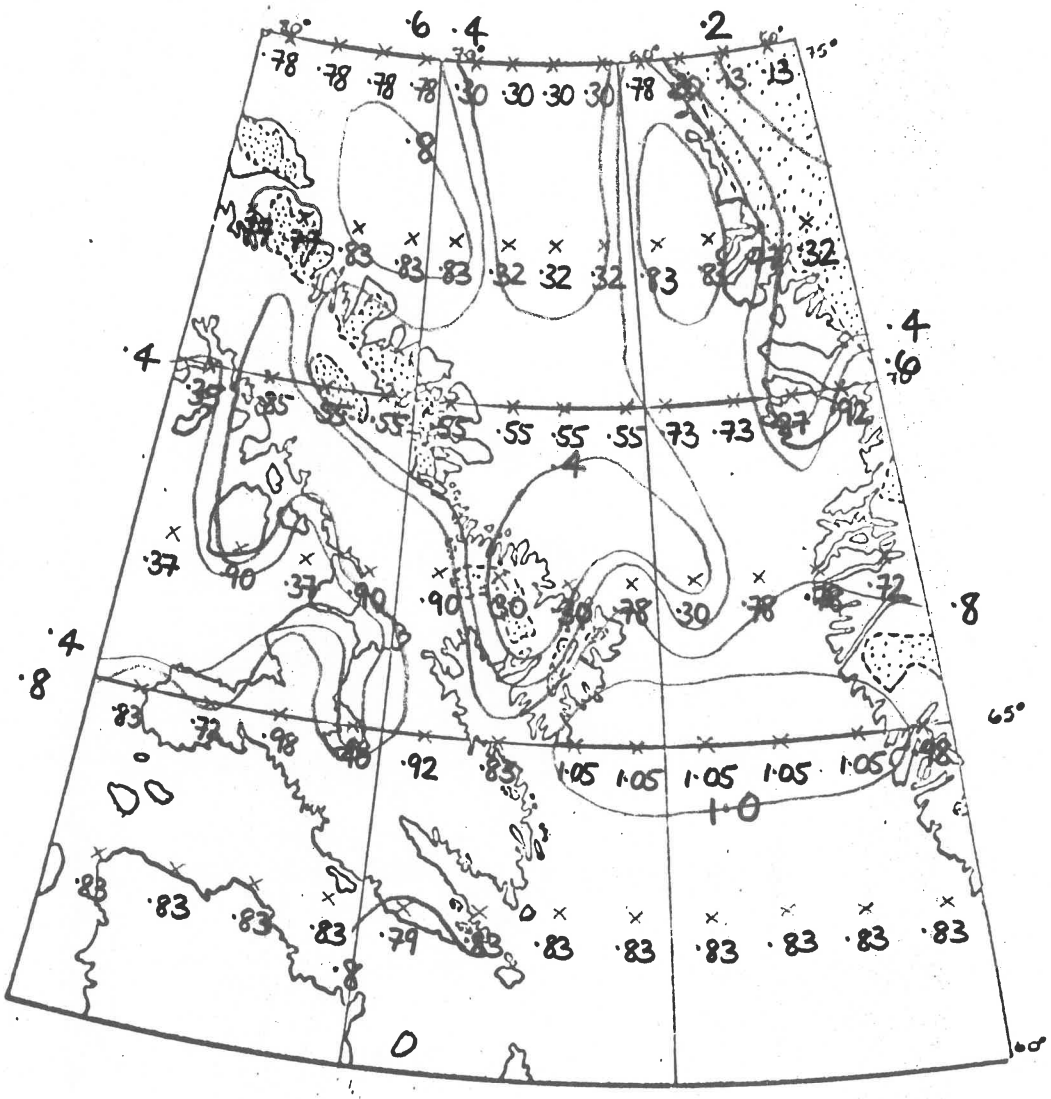

Figure 2.7f 27 July 1970

Table 2.3 Empirical Relations between the Transmitted Solar Radiation (f) and Sine of the Solar Altitude (s) for Categories of Cloud Type and Amount.

$\leq$ 0.25 L, M, H	f = 0.46 + 0.49s
0.26 - 0.61 L	f = 0.45 + 0.24s
0.26 - 1.0 H, L + H, M + H	f = 0.23 + 0.59s
0.62 - 1.0 L	f = 0.12 + 0.22s
0.3 - 0.8 M, L + M	f = 0.13 + 0.16s
0.81 - 1.0 M	f = 0.10 + 0.10s

For atmospheric flux calculations, a single cloud atmosphere was assumed. In this case the flux reaching the surface is composed of three parts: 1) the blackbody flux from the cloud less the amount absorbed between cloud base and ground, 2) that portion of the clear sky flux between the top of the atmosphere and the cloud top which passes through the cloud level (zero in the case of complete cloud cover) and 3) the flux emitted by the layer beneath the cloud. Expressed in terms of a finite difference solution of the radiative transfer equation, this becomes

$$L\downarrow = c\sigma T_c^4 \left(1 - \sum_1^{c-1} \Delta\bar{\varepsilon}_i\right)$$

$$+ (1-c) \sum_1^{N} \sigma T_i^4 \Delta\bar{\varepsilon}_i$$

$$+ \sum_1^{c-1} \sigma T_i^4 \Delta\bar{\varepsilon}_i$$

where the subscripts in the summations represent 12 successive slabs (pressure level increments) from the surface to 20 mb, c is the fractional amount of cloud cover, T_i is the mean temperature (°K), T_c is the mean temperature of the layer in which the cloud is located, and $\bar{\varepsilon}_i$ the mean flux emissivity of the ith slab. The flux emissivity for water vapor is expressed empirically by Sasamori (1968) as

$$\bar{\varepsilon}_i = 0.240 \log_{10} (u_i + 0.010) + 0.622$$

where u_i is the optical thickness (g cm^{-2} H_2O). The effect of carbon dioxide is an order of magnitude less than that of water vapor, and is disregarded in the present study. L↓ was calculated at each point for which a SIRS profile was given, as well as for the radiosonde stations. Extrapolations to grid points were made on the basis of cloud distribution determined from the imagery.

The terrestrial flux L↑ was calculated from the surface temperature maps, with a blackbody flux assumed. Where cloud cover existed, the surface temperature was taken to be 273°K, a reasonable guess for snow, ice, and water surfaces in the summer months. A 1°K error in temperature near 273°K means about a 1 per cent error in the calculated flux.

The sum of the absorbed shortwave term $S\downarrow(1 - \alpha)$ and net longwave term L↓ - L↑ gives the net radiation at the surface R_n. Figures 2.8 a-d illustrate the mapping of R_n.

In order to complete the energy budget calculations, some estimate of the turbulent terms H and LE is required. Using surface pressure maps (Atmospheric Environment Service, Canada), air temperature and

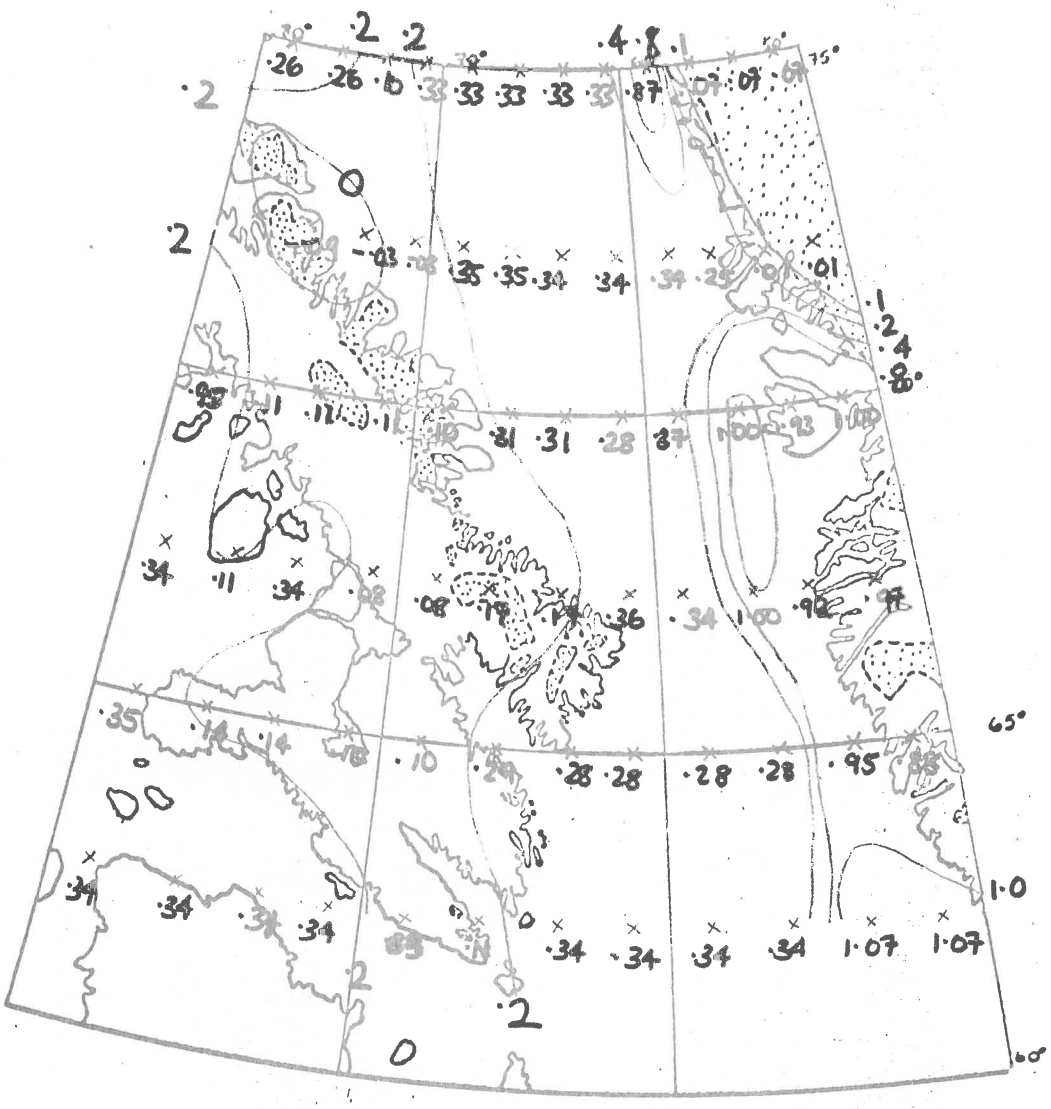

Figure 2.8a 26 June 1970

Figure 2.8 a-d

Regional radiation budget estimates at mid-day (cal $cm^{-2}min^{-1}$) for selected dates from satellite data. 27 June and 8 July are not included since these are almost identical with the maps of absorbed solar radiation.

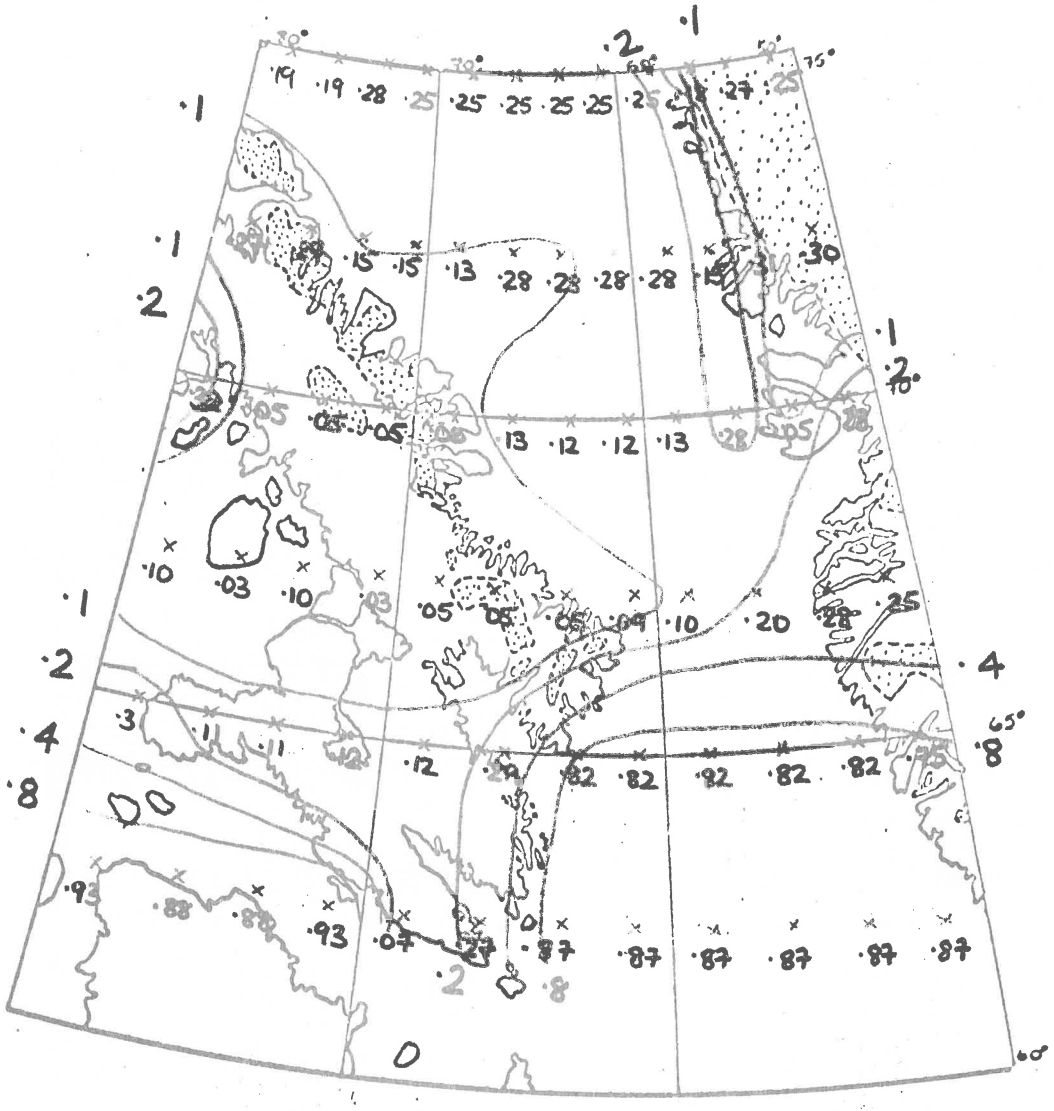

Figure 2.8b 2 July 1970

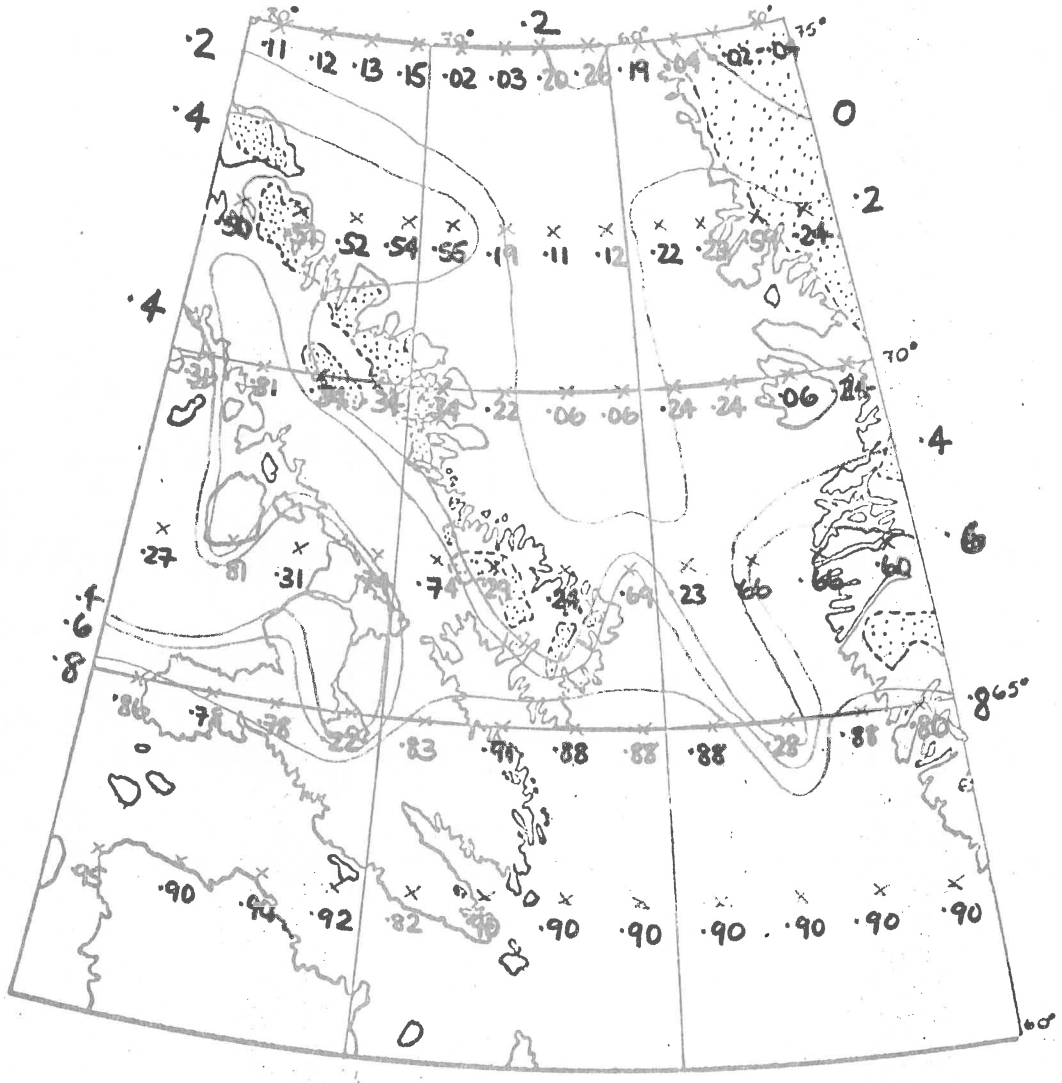

Figure 2.8c 26 July 1970

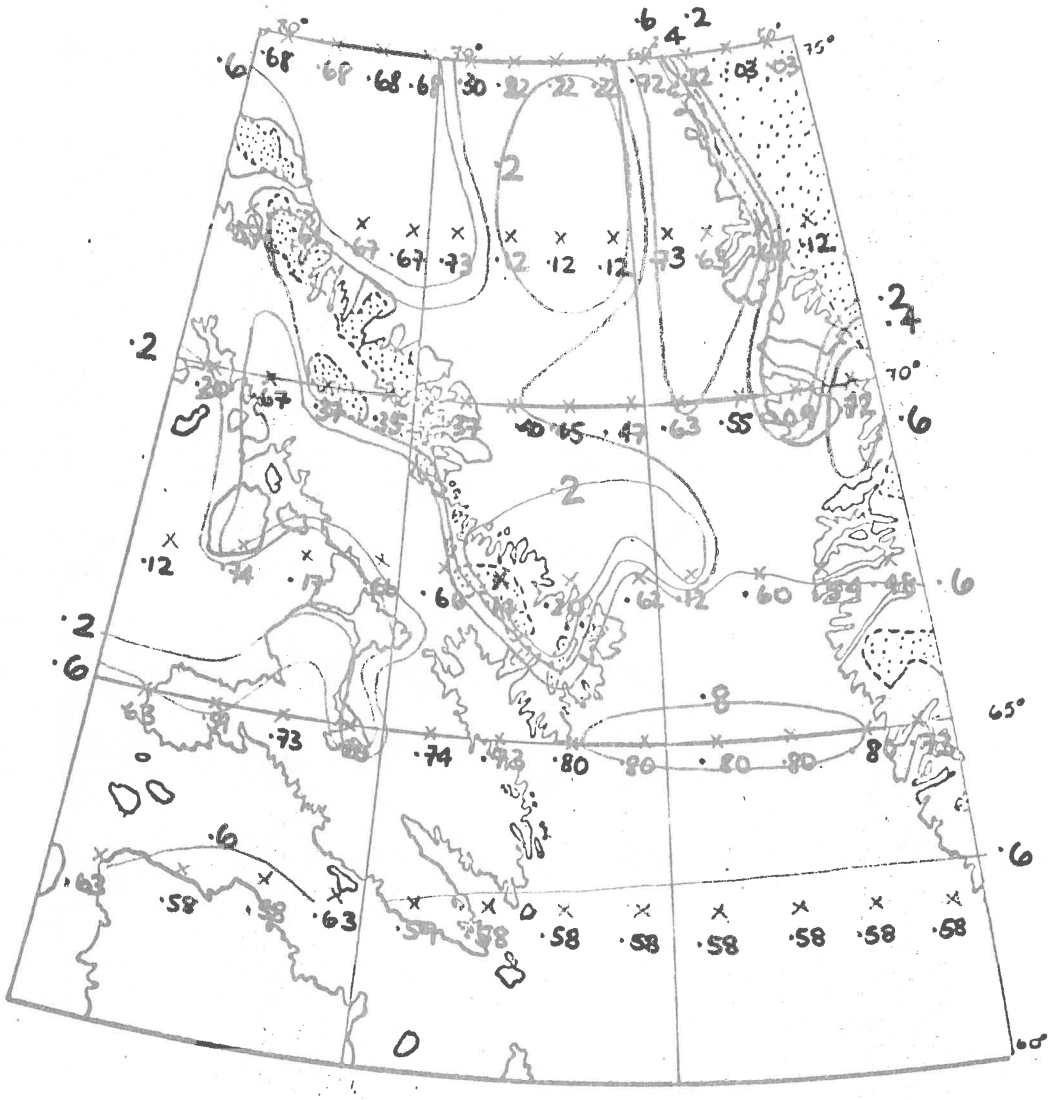

Figure 2.8d 27 July 1970

mixing ratio at 10m were inferred; and a simple extrapolation from the geostrophic wind was employed to provide a 10m windspeed (Hasse and Wagner, 1971). A surface temperature of 0°C was assumed. No attempt was made to provide for a wide range of stabilities in the calculations, rather a logarithmic wind profile was assumed. This is consistent with our own experience over snow and ice surfaces and with the general conclusions of other workers (Grainger and Lister, 1966). A roughness length of 10^{-3}m was chosen as a compromise between somewhat greater values for water and lesser values for snow and ice. Although not done in this study, particular values of roughness length might be assigned to each grid point in accordance with the type of surface at that point.

The following formulae are used in the calculations:

$$A = \frac{k_o^2 \, u_1 z_1}{\log_e (z_1/z_o)}$$

gives the coefficient of eddy viscosity, where k_o is von Kárman's constant (0.41), u_1 is the windspeed at the reference height z_1, and z_o is the roughness length.

The sensible heat flux is given by

$$H = A(\rho c_p) \frac{T_1 - T_o}{z_1}$$

where T_1 is the temperature at the reference height, T_o the surface temperature, and ρ and c_p the density and specific heat of air respectively. The latent heat flux is

$$LE = \frac{AL(0.623\rho)}{p_1} \frac{e_1 - e_o}{z_1}$$

where L is the latent heat of vaporization, p_1 the atmospheric pressure, e_1 the vapor pressure at z_1, and e_o the (saturation) vapor pressure of the ice water surface at T_o.

The combined radiation and turbulent heat budgets (Figures 2.9 a-f) represent the average amount of heat exchanged with the surface (cal $cm^{-2}min^{-1}$) at the time of observations, taken to be local noon. The values shown are indicative of the regime which is characteristic of the synoptic type (Table 2.4) considered. Given at least two satellite passes per day, or a suitable empirical expression for the typical diurnal regime of each budget component, a daily budget could be approximated.

Table 2.4 Synoptic Types for Illustrative Days (after Barry, 1972)

Date	Type	Synoptic Situation
1970		
June 26	532	Cyclonic Control - Davis Str. low and Baffin Bay trough
28	320	Mixed Control - Ridge with trough over Hudson Strait
July 2	521	Mixed Control - Ridge with trough in Baffin Bay
8	310	Anticyclonic Control - Ridge with lows to south
26	310	Anticyclonic Control - Ridge with lows to south
27	410	Anticyclonic Control - High over Baffin Bay, lows to west

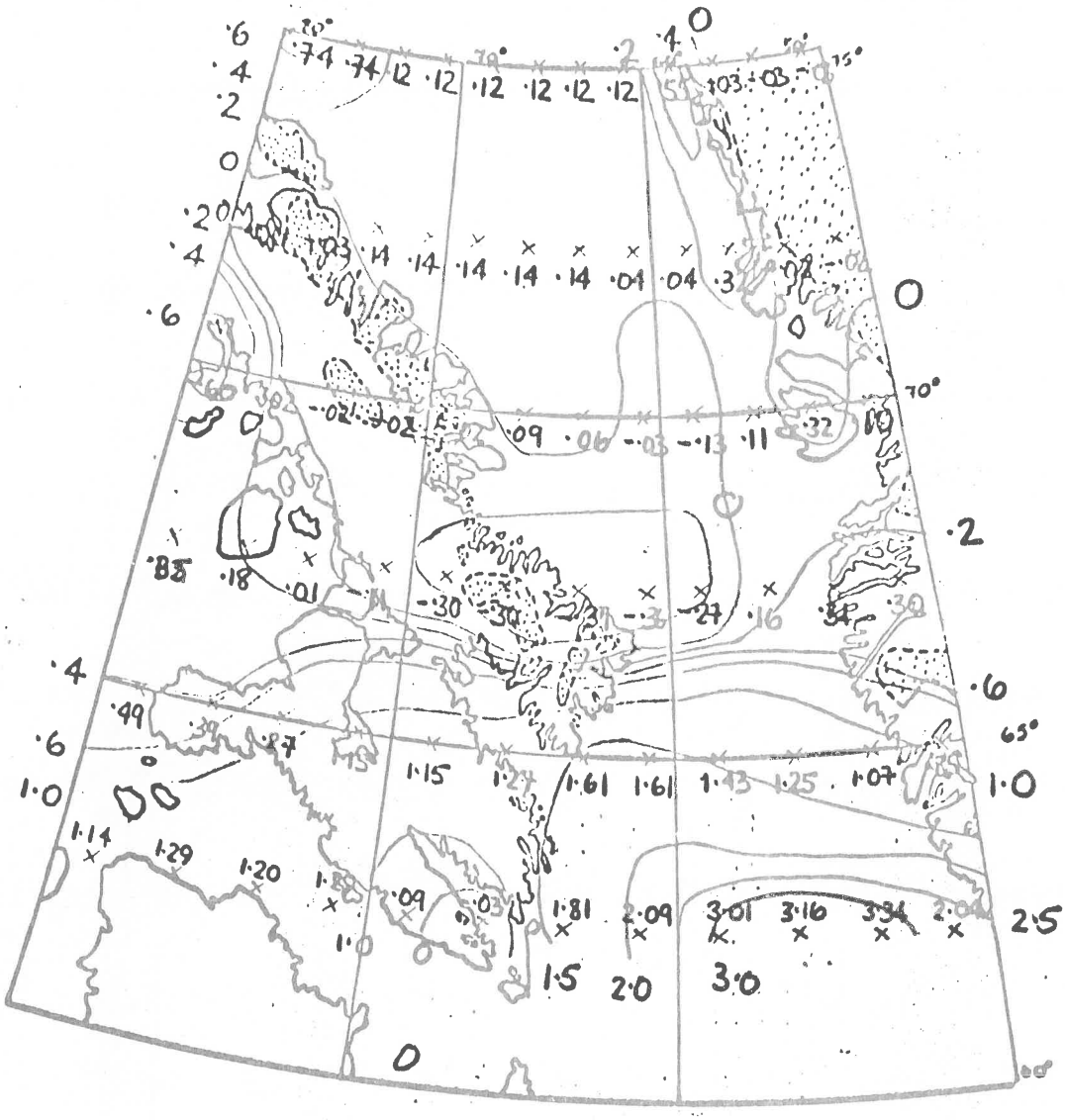

Figure 2.9a 26 June

Figure 2.9 a-f.

Regional energy budget estimates at mid-day (cal $cm^{-2}_{min^{-1}}$) for selected dates from satellite and synoptic data.

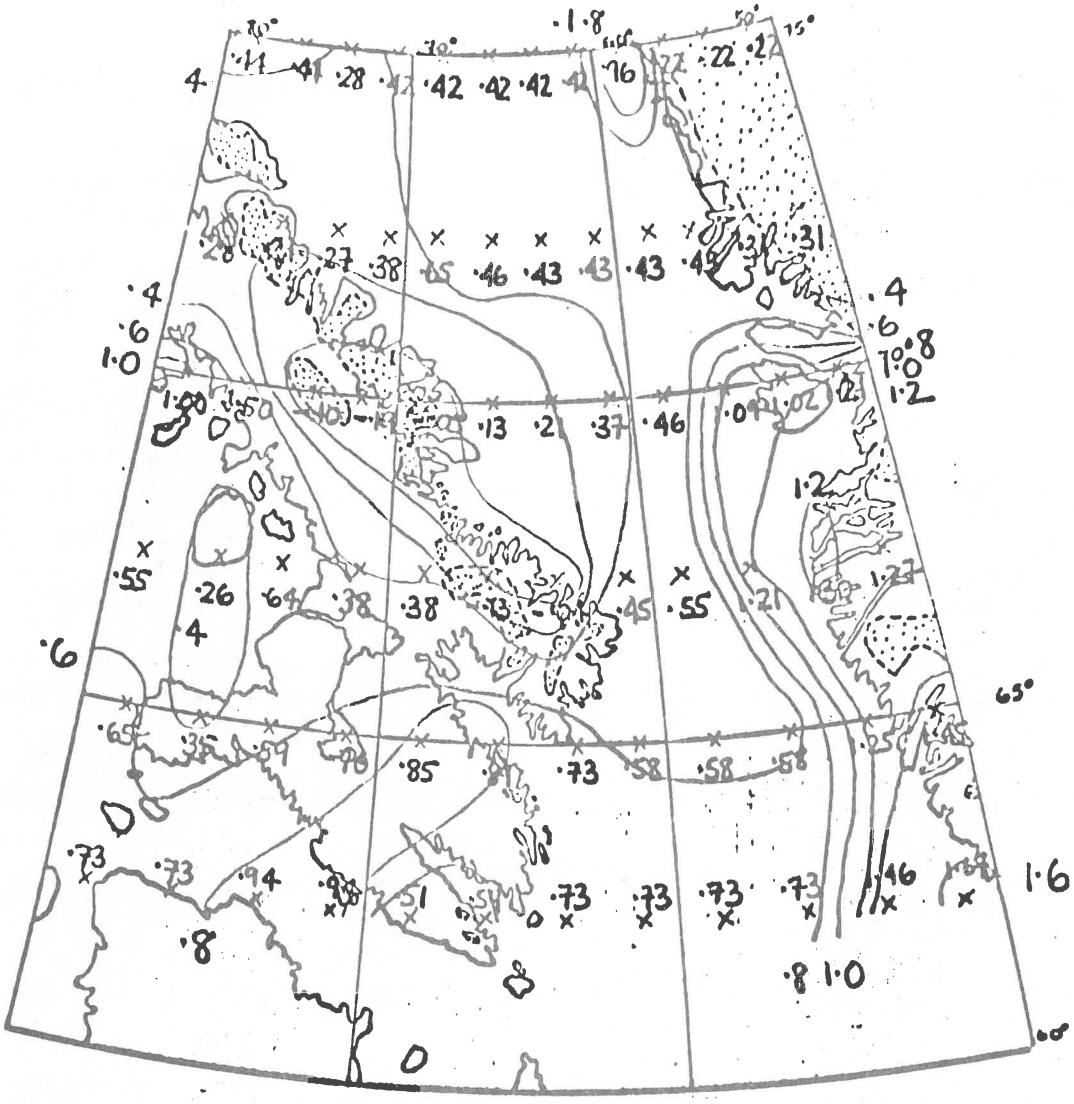

Figure 2.9b 28 June

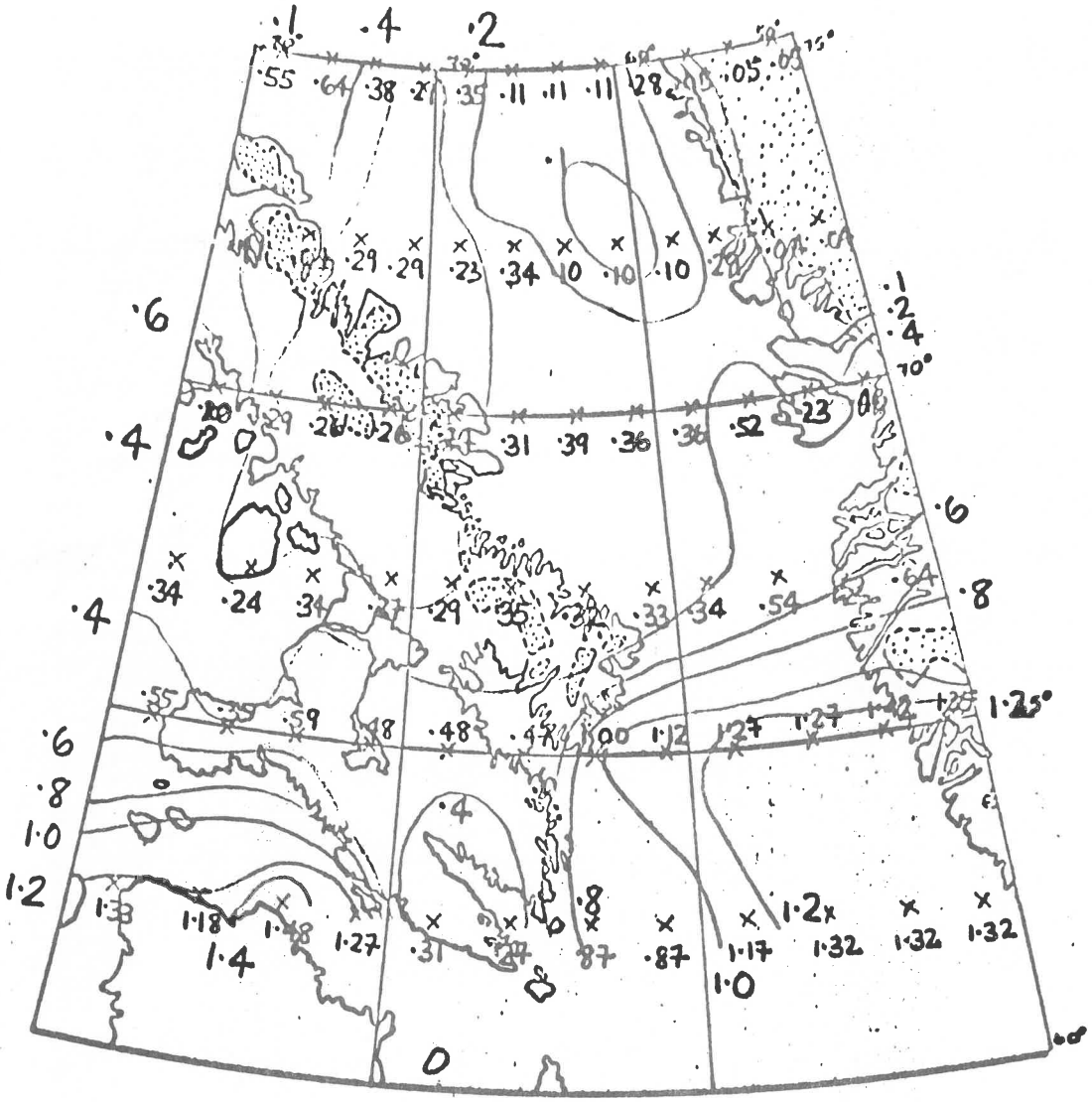

Figure 2.9c 2 July

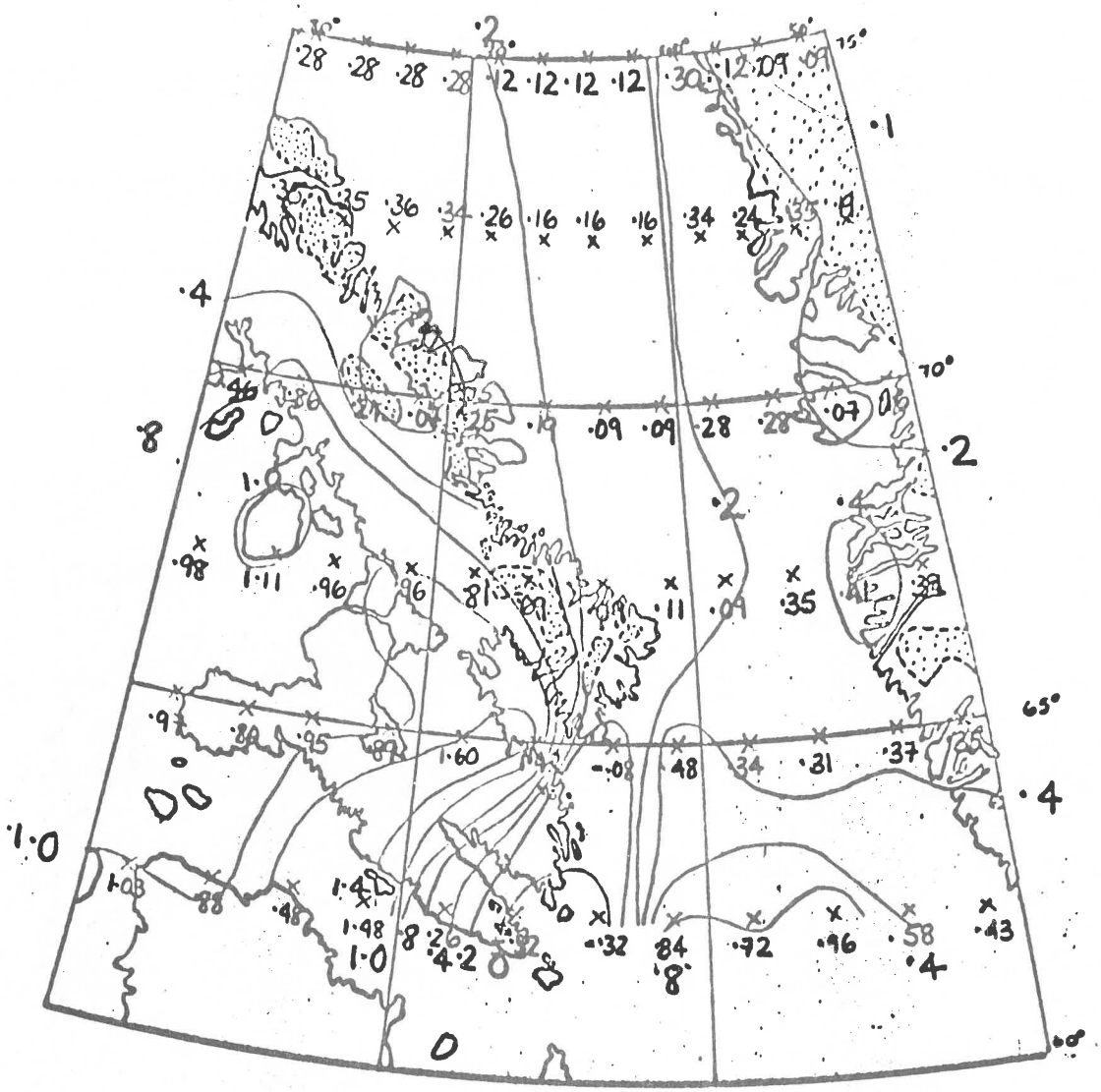

Figure 2.9d 8 July

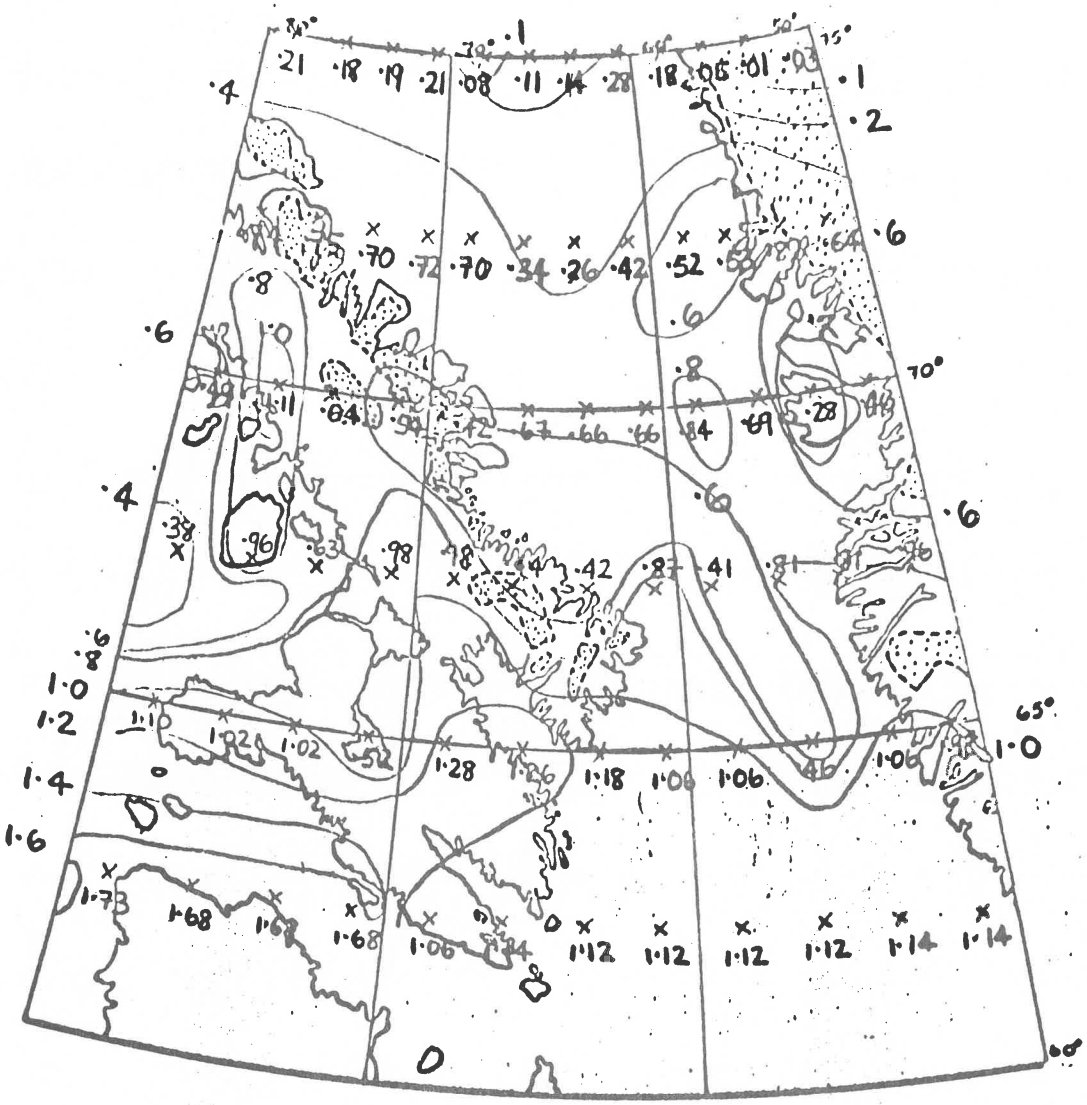

Figure 2.9e 26 July

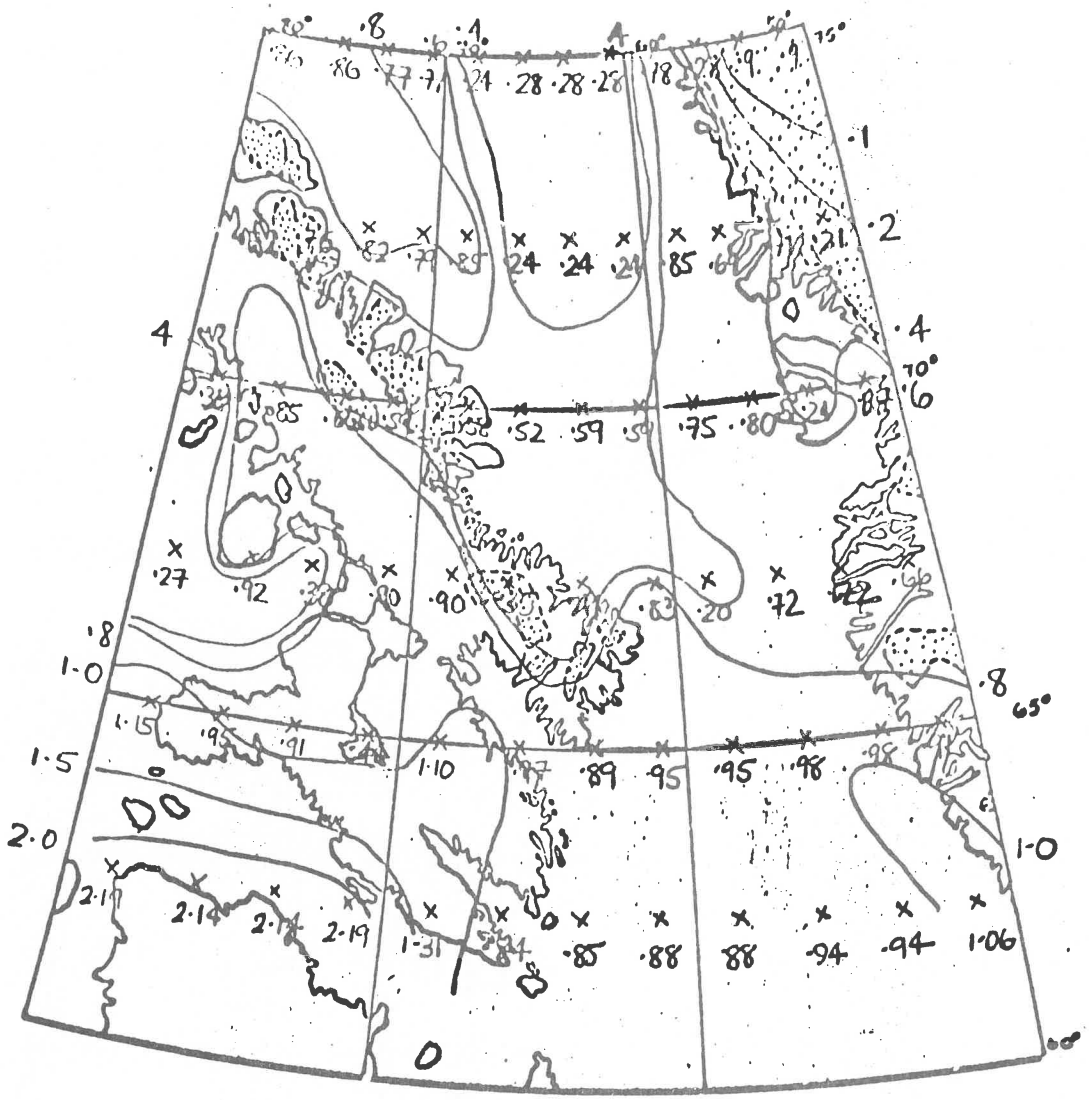

Figure 2.9f 27 July

The usefulness of the satellite data, supported by synoptic information, in mapping regional variations in the energy budget components, is demonstrated by Figures 2-7, 2-8, and 2-9. For example, on June 26th, with a low center in Davis Strait and a trough extending northward, the effects of cloud cover, high albedo and northerly airflow combine to give negative net fluxes over the western Davis Strait area. Conversely, the warm sector of the system over the open water of the Labrador Sea has clear skies and warm air giving rise to a large positive energy flux to the surface. On the same date the North Open Water (northern Baffin Bay) shows substantial heat gain due to its low albedo, in spite of air temperatures around -2°C.

Generally, under conditions of anticyclonic control, albedo is the dominant factor determining the energy flux at the surface, as illustrated over Baffin Island on June 28th (Figure 2-9b). Even with low albedo, however, the maximum mid-day radiation flux will not greatly exceed 1 cal $cm^{-2}min^{-1}$ (cf. Figure 2-8 b, c). Turbulent fluxes may be several times that amount and, although these may be positive or negative, it does not follow that the net long-term average of turbulent fluxes for a particular area will be zero. Thus, Hudson Strait in all of the cases shown, exhibits a consistently large positive turbulent flux. This clearly has some bearing on the relatively rapid recession of the sea-ice shown by Figure 2.5g, although current movements will enhance the break-up. In the Home Bay-Cumberland Peninsula area of Baffin Bay the energy budgets show the opposite effect.

While the energy budget characteristics of the various synoptic types largely conform to what one would infer from cloud and airflow

patterns, within-type variations may be large. For example, the synoptic type designations for July 8th and 26th are the same, but considerably lower temperatures and greater cloud cover on the 8th result in large differences in the respective energy budgets. This suggests the necessity for a more careful look at the synoptic patterns in terms of their cloud patterns and energy budget characteristics. The types on the selected dates represent 15% of all types for July-August 1961-70 and 33% of the major groups of types in these months (Barry, 1972). Continuing analysis of additional days in 1970 for which data are available (and subsequent years) will provide a fuller picture of the synoptic variability of energy budgets.

3. MESOSCALE STUDIES WITH AIRCRAFT AND GROUND TRUTH

3.1 Introduction

The basis for the regional energy budget model is provided by field measurements at the surface under a variety of synoptic conditions. The large step between such measurements and what is seen on the regional scale in the satellite and synoptic data is made on the assumption that conditions are fairly homogeneous in a spatial sense. That is, such parameters as surface albedo, for example, will have approximately the same values for a particular surface type throughout the region at a particular time. Estimates of errors due to spatial variability can be made on the basis of measurements from aircraft in conjunction with surface observations and data from satellites. In addition to providing information on the range of uncertainty in regional budget estimates, combined satellite, aircraft, and surface-based studies provide information on a variety of factors affecting exchange processes such as the radiative properties of clouds, surface and cloudtop albedos, and diurnal surface heating effects.

3.2 Aircraft Measurements Program

During 19-26 May, 1971, a series of flights was carried out in the Baffin Island region for the purposes described in the foregoing paragraph.[1] A total of 11 research flights were made over the Davis Strait and the eastern Cumberland Peninsula in the period 19-26 May.

---

[1] This flight program was supported by NSF under grant number GV 28218. Aircraft support was provided by the Research Aviation Facility, National Center for Atmospheric Research.

Most of the flight tracks were due east-west roughly along the Arctic Circle from Cape Dyer to the open water of the West Greenland Current. Figure 3.1 illustrates the flight track and surface types encountered. A "standard" altitude of 1000 ft. was generally used. The airplane, a Beech Queenair, was equipped with precision pyranometers (top and bottom), a linear net radiometer, and a downward looking radiation thermometer (Barnes PRT-5). Other measurements provided for were relative wind velocity, air temperature and dew point.

The weather systems affecting the area were relatively weak until 26 May. A surface low moved from Hudson Strait on 18 May to the northern Labrador Sea area on the 19th, associated with a 500 mb center over Baffin Bay . From 20-22 May the pattern was anticyclonic over Baffin Island with a weak trough over western Greenland, giving northeasterly circulation over Davis Strait. This high was stronger on the 23rd with northerly anticyclonic flow at 500 mb but a surface low crossed Baffin Island from the west on 24-25 May, and the upper flow became westerly. A more intense system developed over the northern Labrador Sea - Davis Strait on 27th May. Temperatures ranged from a minimum -17°C on 24 May to a maximum of 5°C on 21 May. There was light snowfall on 20 and 21 May (0.05 cm and 0.10 cm w.e., respectively) and 0.33 cm on 26 May. Thus, in general, no great synoptic contrast was experienced, although the flight period fell between major storms on 14-15 May (with 0.96 cm w.e. at Cape Dyer) and 27-28 May (with 0.74 cm w.e. at Cape Dyer).

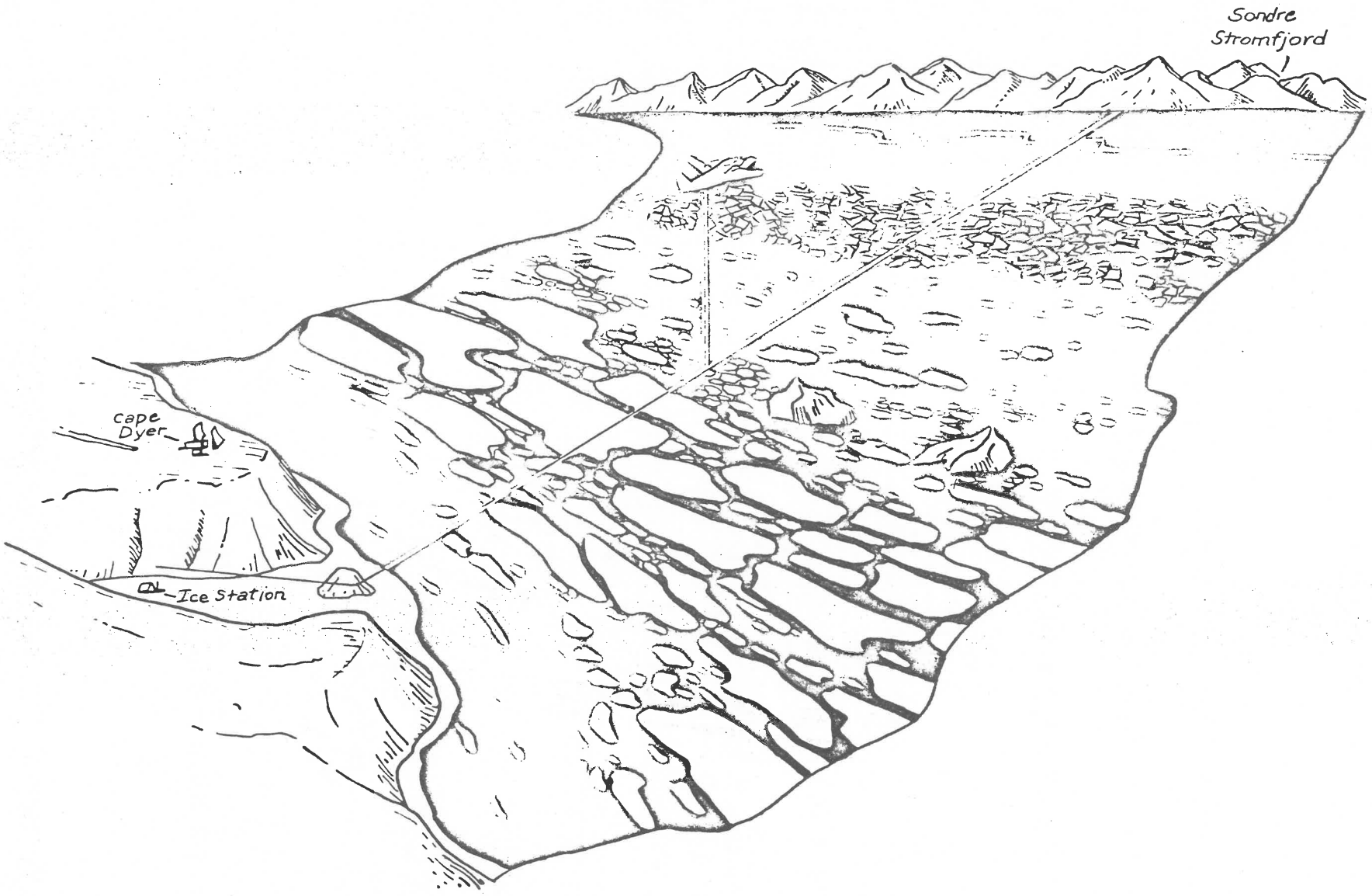

Figure 3.1 Flight track and typical surface conditions over Davis Strait for flight series, 19-26 May 1971.

A micrometeorological station operated on the fast ice in Sunneshine Fiord, below Cape Dyer, provided the basis for surface energy budget calculations. Daily totals of the energy budget components for this site are shown in Figure 3.2. Comparisons between these values and corresponding values from the aircraft measurements provides an indication of the spatial variability for the period. In this comparison, only the radiative terms were considered because of uncertainties in doppler radar wind measurements. (The system frequently went "into memory" due to the absence of signal over smooth ice or water surfaces.) Except for one day during the flight series, snow surface temperatures remained below the melting point, and the snowpack did not become isothermal until some five days after the flights ended. IR temperatures over the sea ice similarly showed that no significant ablation was taking place anywhere on the ice, although some signs of slight surface melting were observed on the last flight.

During each flight at least one pass was made over the ice station for purposes of comparison (Table 3.1). Differences were generally well within the range of variability found for a particular surface type for the flight track as a whole.

Atmospheric and surface sections for two consecutive days of the flight period, shown in Figures 3.3a and 3.3b are illustrative of differing synoptic situations: high pressure on the 25th accompanied by mostly clear skies, and a trough on the 26th associated with deteriorating conditions. Estimated daily energy budgets are

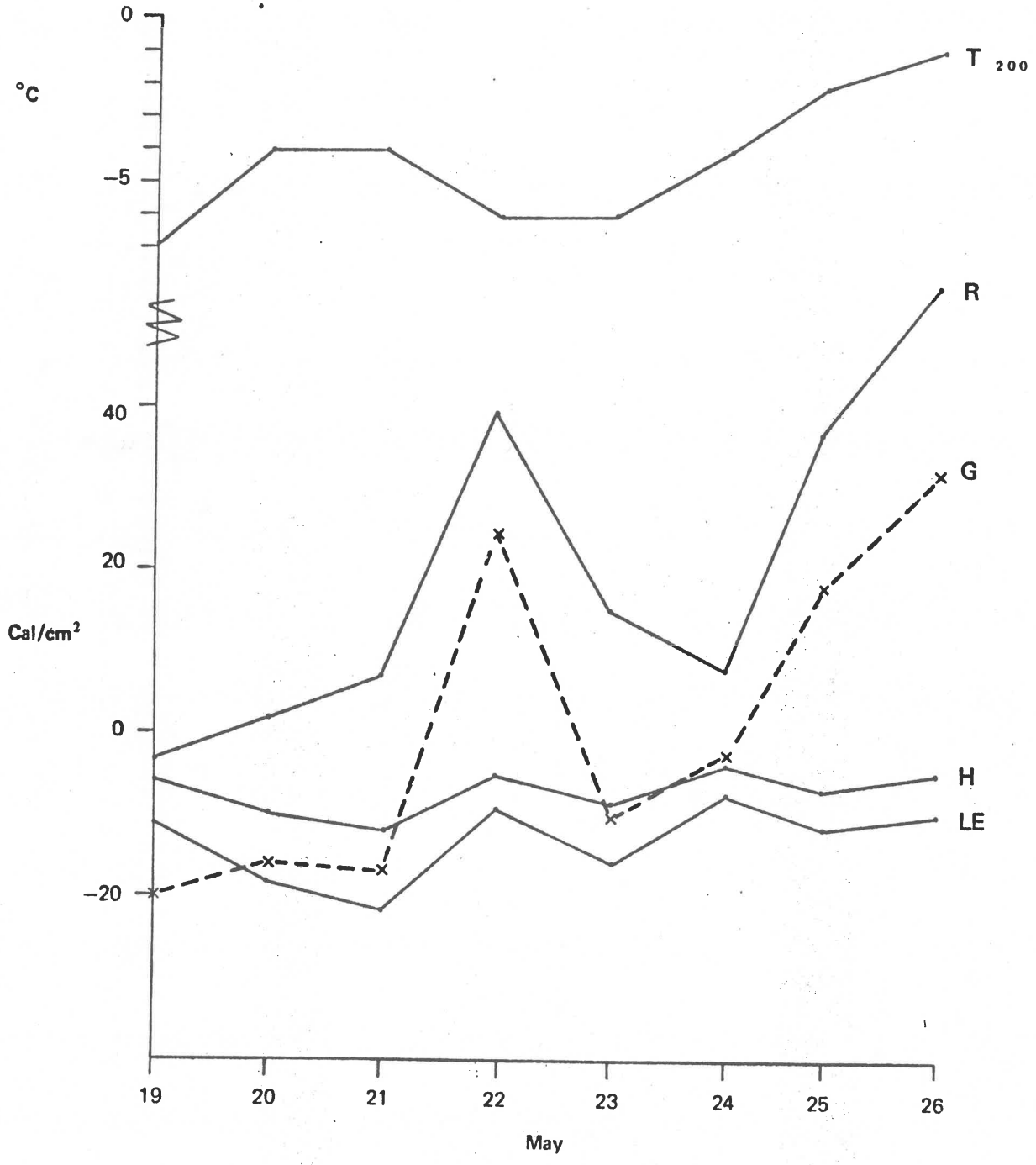

Fig. 3.2 **ENERGY BUDGET COMPONENTS**, FIORD ICE STATION, CAPE DYER ($calcm^{-2}day^{-1}$)

Table 3.1: Comparison of Airborne and Surface Measurements at Fiord Station

Flight No.	Time (EST)	Alt. (feet)	Net Radiation ($cal\text{-}cm^{-2}min^{-1}$)		Solar Flux ($cal\text{-}cm^{-2}min^{-1}$)		Albedo		Surface Temp. (°C)	
			Sfc	Air	Sfc	Air	Sfc	Air	IR	Thermistor
1	0920	300	0.07	0.08	1.03	1.01	.86	.93	-2.9	----
2	1900	500	-0.09	-0.10	0.08	.10	----	----	-6.9	----
	2010	50	-0.08	-0.08	----	.02	----	----	-7.6	----
3	2107	1000	-0.03	0.03	----	.02	----	----	-6.1	----
5	1125	500	0.17	0.28	1.15	1.17	.81	.71	-2.7	(-2.1)
7	1140	1000	0.18	0.17	1.18	1.05	.83	.82	-0.8	-0.6
8	1201	1000	0.12	0.13	1.02	1.01	.80	.82	-0.5	0.0
9	1015	100	0.14	0.16	1.08	1.04	.77	.78	-0.4	-0.4
	1259	100	0.19	0.22	1.12	.86	.77	.75	-0.6	----
10	2147	200	-0.06	-0.03	----	----	----	----	-2.9	-2.4
	0003	1000	-0.04	-0.02	----	----	----	----	-3.8	----
11	1021	100	0.12	0.18	0.86	0.78	.82	.83	0.2	0.0

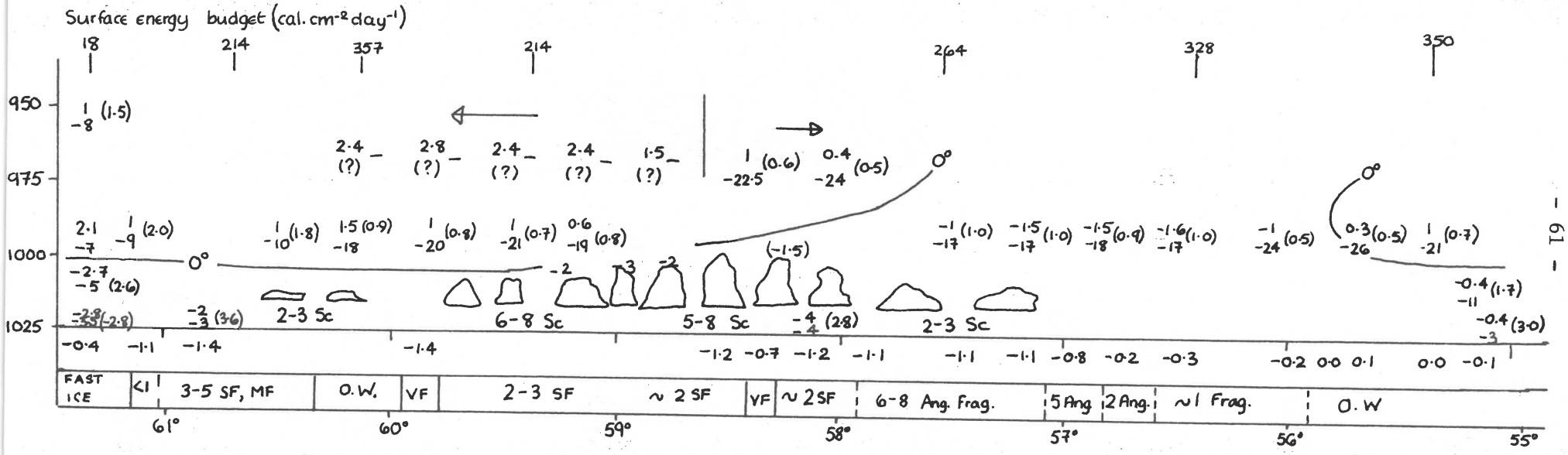

Figure 3.3a

Atmospheric and surface cross-section for Davis Strait, 25 May 1971; anticyclonic situation.

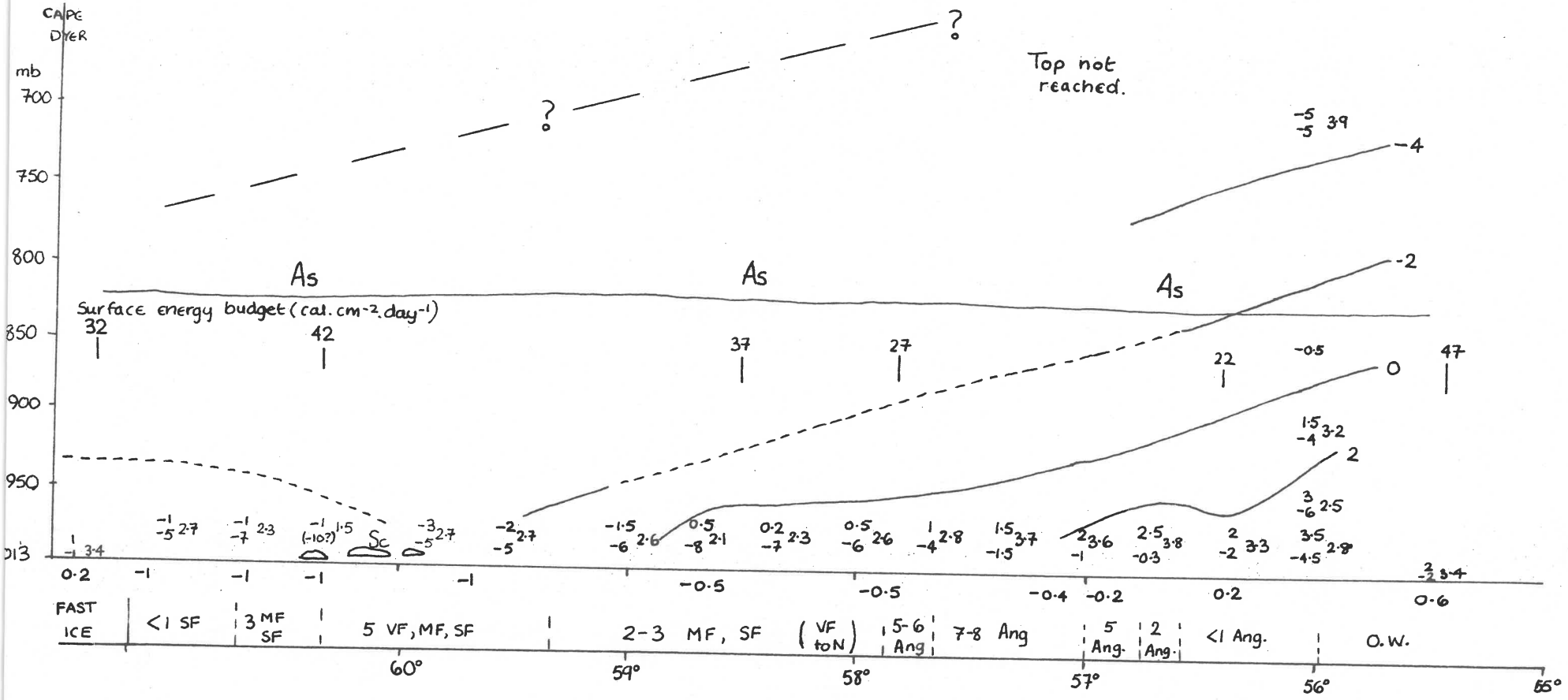

Figure 3.3b

Atmospheric and surface cross-section for Davis Strait, 26 May 1971; cyclonic situation.

shown for several parts of the track. Using the surface station values as an index (Fig. 3.2), these totals were calculated on the assumption that the synoptic situation remained unchanged throughout the day and that net radiation was the only term that varied across the track. Differences in the daily budget were based upon the daytime (06 to 18 hrs LST) portion of the net radiation curve, variations having been found to be small on nighttime flights. A daily total for a particular part of the track was found by multiplying the daytime total for the ice station by the ratio of measured midday values for the two surfaces and subtracting from this the nighttime total for the ice station. This approach tends to exaggerate the contrast between clear and heavily overcast days. However, it should be noted that the range of albedos for the track was from near 0.90 for fast ice to 0.04 for open water, and the effect of cloud on the radiation budget will be quite large in terms of absolute values for the latter.

Obviously variations in turbulent and longwave flux terms must be considered in a complete treatment of the problem. However, the results shown tend to confirm the validity of regional extrapolations based upon known differences in air and surface temperatures, cloud cover, and surface and cloudtop albedos.

3.3 Satellite and Aircraft Data Comparisons

Satellite data covering the May, 1971 flight period included Nimbus-4 IDCS imagery and ITOS-1 IR temperature maps and small-scale imagery. Flights usually took place within one or two hours of a satellite pass.

The visual imagery revealed that ice conditions along the flight track were somewhat lighter than to the north or south (Figure 3.4). No significant change in sea ice distribution was noted during the period. Also determined from a comparison of flight logs with the visual imagery was the fact that as much as 6 tenths thin, semi-transparent stratus over the pack was not visible in the pictures and that the lower limit of detectable ice coverage seems to be 2 to 3 tenths. Color enhancement techniques[1] were applied to the films with some success in that, for those days known to be clear, the proportions of various pack densities could be estimated quite closely (Table 3.2). The problem of distinguishing low stratus over open water from open pack conditions still remains, however.

The 1:4 million IR temperature maps provide some 25 temperature values for the line extending across Davis Strait from Cape Dyer. For clear or scattered cloud conditions, satellite temperatures usually agreed well with those measured in flight. Since the ITOS-1 temperatures are in 2°K steps, a close comparison cannot be made. However, as Table 3.3 shows, agreement is within the range of uncertainty of the satellite data.

No attempt was made to calculate regional budgets for the period from satellite data alone, since SIRS profiles were not obtainable. In view of the close agreement between satellite data interpretations

---

[1] A color enhancement system (Spatial Data Systems Model 704) was recently obtained by INSTAAR in connection with a NASA ERTS-A contract. This arrived too late to be useful in the initial Baffin study but it is apparent that application of this system will permit better resolution of cloud and surface features in the satellite imagery.

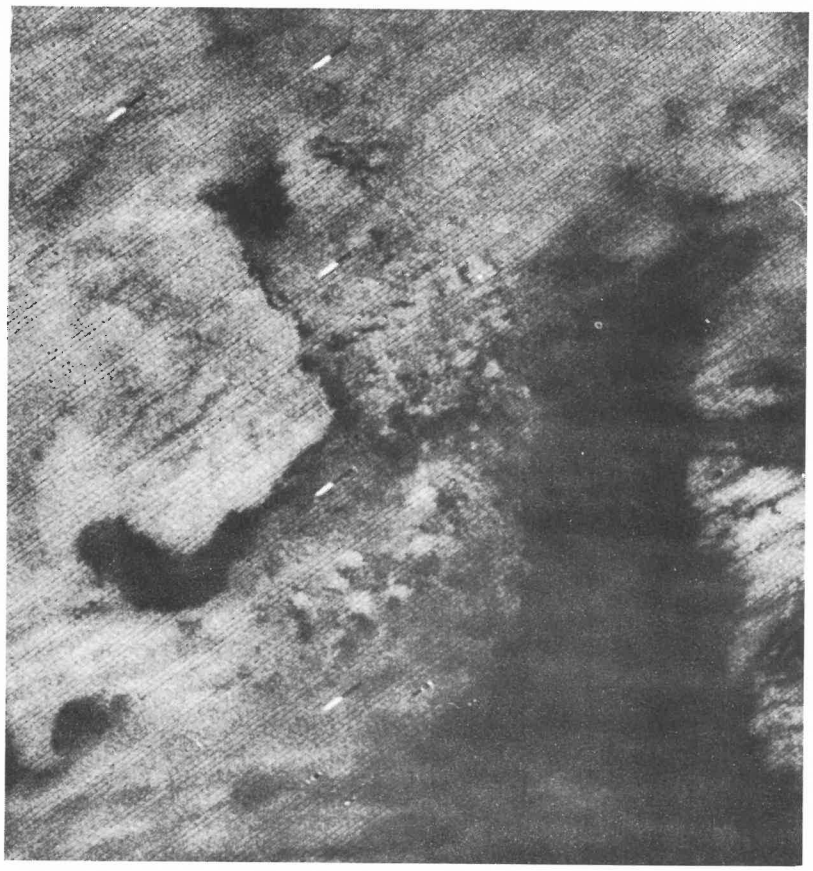

Figure 3.4

Nimbus 4 IDCS showing ice conditions in Davis Strait

(25 May 1971)

Table 3.2 A comparison of ice cover estimates for the area 66-67°N by 53-63°W from color-enhanced Nimbus-4 IDCS imagery and observations from aircraft (25 May 1971).

Ice Cover Categories	Per cent Area		Albedo
	Aircraft	Satellite	(Aircraft)
1. Fast ice, 7-8/8 pack and large floes	20	24	.78
2. Close pack (5-6/8)	15	18	.35
3. Open pack (2-4/8)	28	15	.22
4. Open water (< 1/8)	37	39	.07

and flight observations, it is felt such calculations would be reasonably good.

3.3 Variability of Energy Budget Parameters in Space and Time

One of the objectives of the flight program was to provide information on the degree of variability of the various energy budget terms over the region. To some degree, the satellite data can also be used for this purpose. A first attempt at such estimates from aircraft data is shown in Table 3.4 where air temperature, surface (IR) temperature, and net radiation were averaged for the 300 km track across Davis Strait. In view of the comparative diversity of surface features along the track (fast ice to open water), the amount of variability is quite low. These values, then, may be taken as indicative of the range of possible error in radiation budget estimates for a given synoptic situation.

Table 3.3 A Comparison of Surface Temperatures from Aircraft and ITOS-1 Satellite Measurements

	FAST ICE	CLOSE PACK	OPEN PACK	OPEN WATER CANADIAN CURRENT	OPEN WATER WEST GREENLAND CURRENT
Day (1130 EST) Cloud (tenths)	Clear	3 Sc	Clear	3-6 Sc	Clear
Aircraft	272.8	272.2	272.0	271.8	273.0
ITOS-1	272	272	271	272	273
Night (2100 EST) Cloud (tenths)	2Ac 6Cs	5Ac 2Cs	5Ac 2Cs	5Ac 2Cs	5Ac 2Cs
Aircraft	270.7	271.6	271.9	272.0	272.8
ITOS-1	272	270	272	272	272
Nocturnal Cooling	-2.1	-0.6	-0.1	(+ 0.2)	-0.2

Table 3.4 Averages and Standard Deviations of Essential Energy Budget Parameters for the Flight Track across Davis Strait

FLIGHT	Air Temp. (300 m) Mean	Stand. Dev.	Surface Temp. Mean	Stand. Dev.	Net Rad. (300 m) Mean	Stand. Dev.
May 20 Night	-6.4	0.2	-2.9	2.1	-0.06	0.03
24 Day	-7.3	0.6	-1.5	0.4	0.64	0.19
25 Day	-0.1	1.2	-1.4	0.7	0.64	0.20
25 Night	1.9	1.2	-1.6	0.4	-0.02	0.01
26 Day	0.5	1.8	-0.8	0.4	0.17	0.06
	(°C)		(°C)		(cal $-cm^{-2}-min^{-1}$)	

The within-type variability is suggested by a flight sequence over a 50 km stretch of uniform fast ice (Table 3.5). In this case surface cooling associated with a decrease in net radiation led to a change in surface temperature of 0.6°K in about an hour. Such a change is probably predictable since it is associated with the normal diurnal variation in net radiation. Even with air temperatures above freezing, it is common for temperatures of snow and ice surfaces to fall below freezing due to radiative cooling. Thus, for any sea ice surface a diurnal temperature variation of several degrees is to be expected on all but the warmest days. Well-mixed ocean water shows little diurnal variation in surface temperatures, and Barnes, et al. (1972) have used this fact to distinguish between sea ice and open water by comparing day- and night-time IR imagery for the same area.

In moderately close to close pack ice a diurnal temperature effect is observed in the water. Figure 3.5 shows two near-surface profiles measured in close succession within pack ice and in an extensive open water area adjacent to the pack. The excessive heating of the near surface water, also observed to a lesser degree in melt-water puddles, serves to raise the apparent temperature of the pack when viewed remotely. The apparent temperature T_A can be expressed in terms of the amount of ice C (tenths) and the surface temperatures of the ice T_i and water T_w respectively as

$$T_A = [CT_i^4 + (1-C)\ T_w^4]^{1/4}.$$

Using the aircraft-derived temperatures of Table 3.3, apparent temperatures have been calculated as shown in Table 3.6 .

Table 3.5 Short-term change in fast ice surface temperature (22 May 1971: Measurements at 300m under 8 tenths Altocumulus.)

Time (LST)	IR (°C)	R_n (Cal-cm^{-2}-min^{-1})
1430	-2.9 ± 0.2	0.13 ± 0.02
1520	-3.6 ± 0.09	0.05 ± 0.01

Table 3.6 Calculated apparent temperatures based upon aircraft measurements

	Day	Night
T_I	272.8 °K	270.7 °K
T_w	271.7	272.0
T_A (3 tenths pack)	272.0	271.6
T_A (7 tenths pack)	272.5	271.1

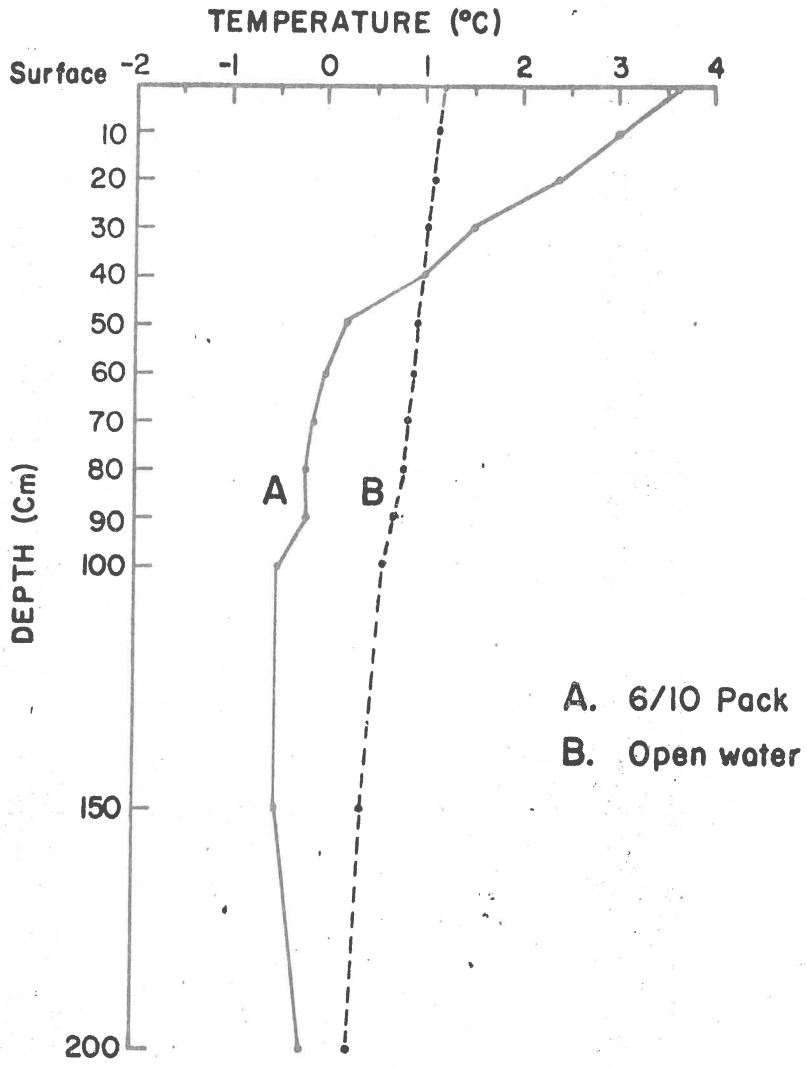

Figure 3.5 .

Near-surface sea temperatures in Davis Strait, off Broughton Island, within and adjacent to close pack ice on a clear July day, near mid-day.

For summer ice temperatures, the differences shown between close and open pack are too small to be resolved with present satellite sensors. In winter, however, when temperature differences of as much as 40°C exist between open water and ice surfaces, this method might be used to estimate pack density.

Summer observations at Broughton Island, 180 km northwest of Cape Dyer, in 1971 and 1972 provide a further basis for comparison of satellite and surface measurements. Complete energy budgets are being calculated on a daily basis in relation to synoptic conditions and the results of this continuing program will be used to construct an energy budget climatology for the region. Visual imagery and IR maps are being examined in the process. A preliminary inspection was made of IR data for three consecutive ITOS-1 passes which coincided with clear sky conditions. For a transect eastwards from Broughton Island to 60°W, over which region Canadian Ice Patrol reports showed > 9 tenths ice cover, extremely uniform surface temperatures prevailed (Table 3.7). At that time, melting of snow cover on the fast ice was well developed with 1 to 3 tenths puddling observed in the vicinity of Broughton Island. Several open water areas of considerable extent were visible in ESSA-9 AVCS, but were not detectable in the IR maps.

3.4 Effects of Cloud

As shown in the discussion of regional energy budgets (Section 2), satellite IR data were useful in determining the amount and extent of cloud cover. The radiative characteristics of relatively thin, cold arctic clouds are complex, however, and more needs to be learnt

Table 3.7 Mean satellite-derived surface temperatures at 67.5°N for three consecutive passes.

	$\bar{T}$ (°K)	σ(°K) (n = 16)
July 7 (Day)	274	2
July 7 (Night)	274	2
July 8 (Day)	275	1

of their properties before satellite observations can be confidently used. It has been found, for example, that the blackbody assumption is inadequate in the case of arctic stratus (Marshunova and Chernigovskiy, 1966), a fact well known for cirrus clouds. Thus when a satellite radiometer views a typical cloud situation in the Arctic, it sees a composite of surface and cloud-top fluxes. For lower level stratus, often located at the top of the surface inversion, the apparent temperature will tend to be close to the actual surface temperature or even greater. This situation leads to confusion in mapping the cloud and in determining actual surface temperatures.

Investigations of clouds in this connection have been of several kinds. During the 1971 flight program, comparisons were made between surface temperatures as measured over the ice station at 200 meters from the aircraft and temperatures seen in that vicinity by ITOS-1 (Table 3.8). Screen temperatures are also shown because of their generally close agreement with surface temperatures. Given sufficient cases of this kind, a statistical relationship between surface

Table 3.8 Comparison of Satellite, Aircraft, and Ground-based Surface Temperatures. Fiord Ice Station below Cape Dyer.

May	LST	Screen (2m)	ITOS-1 (1)	PRT-5	Cloud Conditions
19	00	260	-	-	Clear
	12	270	270	269	1 Sc
20	00	260	268	264	10 Sc (to 1000 m) Opac ≥9
	12	273	264	-	Same
21	00	266	267	271	7-10 Sc (to 500 m) Opac 4-10
	12	274	-	270	Same
22	00	262	261	-	2 Sc
	12	269	256	270	6-10 Sc
23	00	265	251	-	9 Sc
	12	271	-	-	1 Sc
24	00	259	269	-	3 Ac
	12	277	263	273	9 Ac
25	00	267	-	-	3 Ac
	12	276	271	273	3 Sc
26	00	267	272	270	6 Cs 2 Ac
	12	274	242	273	10 As (2000 m)

(1) Mean value of possible range.

temperature "error" and cloud cover can be established. Analysis of 1971 and 1972 data from Broughton Island for this purpose is continuing.

A more direct approach involves radiometric studies of the clouds, both from aircraft and on the ground. Studies of stratiform clouds using a ground based radiometer (PRT-5, 9.5-11.5 μm) were initiated at Broughton Island during the summer of 1972. An improved atmospheric flux model is expected to result from this work.

4. CONCLUSIONS

The applications of satellite data to energy budget calculations in arctic areas has been demonstrated in the foregoing sections. The major achievements can be summarized as follows:

1. Familiarization with the available data and its limitations in relation to the region.
2. The development of interpretive skills and techniques, particularly with respect to visual and IR imagery in arctic areas.
3. Construction of an adequate but flexible regional energy budget model compatible with satellite data.
4. Assessment of the spatial and temporal variability of exchange parameters.
5. Identification of specific problems requiring field investigation; notably, problems associated with low cloud and the inversion.

These accomplishments form the basis of a regional energy budget climatology, which ultimately must be based on a larger number of synoptic cases spread over several years. The work reported here has been based on the first year of satellite data coverage which was available in the requisite variety of forms for arctic energy budget investigations.

Further progress in this direction now depends upon routine analysis of increasingly better satellite data, notably higher resolution infrared coverage with the NOAA satellite series, multispectral, high resolution imagery and ground platform capabilities with ERTS-B, and microwave radiometry in Nimbus E. As these data become available, they will be incorporated within the framework of the ongoing regional study. The summer of 1970 also saw the initiation of a continuing program of field activities in the region of western Davis Strait by the authors and their associates. Subsequent experience indicates that a period of deteriorating climatic conditions is in progress in the region (Bradley and Miller, 1972; Jacobs and Barry, 1972). Satellite studies form an essential part of the continued monitoring of these conditions.

ACKNOWLEDGEMENTS

Support for this study was provided by the Office of Polar Programs, National Science Foundation principally under grant number GV 28220 and the related grant GV 28218. The authors are indebted to the following for data, helpful discussions, and assistance in various forms: The National Space Science Data Center, Goddard; Dr. J.C. Barnes, Mr. J.E. Sissala, and Mr. W. Abbott of the Nimbus Applications Group, Allied Research Associates, Goddard; Dr. E. Paul McClain and Mr. H.M. Woolf of National Environmental Satellite Service, NOAA; Lt. Cdr. W.S. Dehn, U.S. Fleet Weather Facility, Suitland; The National Center for Atmospheric Research, Boulder; and The Atmospheric Environment Service, Canadian Ministry of Environment. Mrs. M. Eccles and Mr. G. Wahlstrom of this Institute assisted in computer programming and data reduction.

References and Bibliography

Aber, P.G., and Vowinckel, E. 1971: Evaluation of north water spring ice cover from satellite photographs. Dept. Meteorol., Publ. No. 101, McGill Univ., Montreal.

Anderson, R.K., Ashman, J., Bittner, F., Farr, G., Ferguson, E., Oliver, V., and Smith, A. 1969: Application of meteorological satellite data in analysis and forecasting. ESSA Technical Rep. NESC 51, Nat. Environmental Satellite Center, Washington.

Andrews, J.T., Barry, R.G., and others, 1972: Present and palaeo-climatic influences on the glacierization and deglacierization of Cumberland Peninsula, Baffin Island, N.W.T., Canada. INSTAAR Occas. Pap. No. 2, University of Colorado, Boulder, 220 pp.

Barnes, J.C., Chang, D.T., and Willand, J.H. 1969: Use of satellite high resolution infrared imagery to map Arctic Sea ice. Final Rept., NASA Contr. NG 2306-68-C-0276, Allied Res. Assoc., Inc. Concord, Mass, 109 pp.

Barnes, J.C., Chang, D.T., and Willand, J.H. 1972a: Image enhancement techniques for improving sea-ice depiction in satellite infrared data. J. Geophys. Res., 77(3), 453-462.

Barnes, J.C., Chang, D.T., and Willand, J.H. 1972b: Application of ITOS and Nimbus infrared measurements to mapping sea ice. Final Report, NASA Contr. No 1-36025, Allied Res. Assoc., Baltimore, Md. 87 pp.

Barry, R.G. 1972: Further climatological studies of Baffin Island, Northwest Territories, Inland Waters Directorate, Tech. Rep. No. 65, Dept. of Environment, Ottawa.

Barry, R.G., and Fogarasi, S. 1968: Climatology studies of Baffin Island,

Northwest Territories. Inland Waters Directorate, Tech. Bull. No. 13, Dept. of Energy, Mines and Resources, Ottawa, 106 pp.

Bradley, R.S., and Miller, G.H. 1972: Recent climatic changes and increased glacierization in the eastern Canadian Arctic. Nature, 237, 285-287.

Dehn, W.S. 1972: Antarctic sea ice forecasting, Antarctic Journal, 8(3), 57-58.

Grainger, M.E., and Lister, H. 1966: Wind speed, stability, and eddy viscosity over melting ice surfaces. J. Glaciol., 6, 101-127.

Hasse, Lutz, and Wagner, V., 1971: On the relationship between geostrophic and surface wind at sea. Mon. Wea. Rev., 99(4), 255-260.

Jacobs, J.D., and Barry, R.G. 1972a: Air-sea interaction studies in Davis Strait, EOS, 53, p. 387 (abstract).

Jacobs, J.D., and Barry, R.G. 1972b: Regional energy budget studies in western Davis Strait. Symp. on Sea-Air Interactions in Polar Regions, Am. Geophys. Union, San Francisco, December 1972.

Marshunova, M.S., and Chernigovskiy, N.T. 1966: Numerical characteristics of the radiation regime in the Soviet Arctic. Proc. Symp. on the Arctic Heat Budget and Atmospheric Circulation. Fletcher, J.O. (ed.), The Rand Corp., Santa Monica, Calif. 279-297.

McClain, E. P., and Baker, D.R. 1969: Experimental large-scale snow and ice mapping with composite minimum brightness charts. NESC TM 12, Nat. Environmental Satellite Center, Washington.

Reynolds, R. 1971: A study of circulation types and energy budgets for the Baffin Island region during June, July, and August, 1970. Unpubl. M.A. Thesis, Dept. Geography, Univ. of Colorado, 74 pp.

Sabatini, R.R. (ed.), 1970: The Nimbus IV User's Guide. Goddard Space Flight

Center, Nat. Aeronautics and Space Administration, Greenbelt, Md. 214 pp.

Sabatini, R.R., Rabchevsky, G.A., and Sissala, J.E. 1971: Nimbus Earth Resources Observations. Tech. Rept. No. 2. Contr. NAS 5-21617 (National Aeronautics and Space Administration), Allied Research Assoc., Inc. Concord, Mass.

Sasamori, T. 1968: The radiative cooling calculation for application to general circulation experiments. J. Appl. Met., 7, 721-729.

Sasamori, T., London, J., and Hoyt, D.V. 1972: Radiation budget of the southern hemisphere, in Meteorology of the Southern Hemisphere. Met. Monogr. (in press).

Saunders, P.M. 1970: Corrections for airborne radiation thermometry. J. Geophys. Res., 75, 7596-7601.

Sellers, W.D. 1965: Physical Climatology. Univ. Chicago Press, Chicago, 272 pp.

Smith, W.L., Woolf, H.M., and Jacob, W.J. 1970: A regression method for obtaining real-time temperature and geopotential height profiles from satellite spectrometer measurements and its application to Nimbus 3 "SIRS" observations. Mon. Wea. Rev., 98(8), 582-603.

Szekielda, K.H., and Mitchell, W.F. 1971: Oceanographic applications of color-enhanced satellite imageries. NASA X-651-71-53, Goddard Space Flight Center.

Vowinckel, E., and Orvig, S. 1969: Climatic change over the Polar Oceans: II a method for calculating synoptic energy budgets. Archiv für Meteorol., Geophys., und Bioklimat, 17, 121-146.

Warnecke, G., Allison, L.J., McMillin, L.M., and Szekielda, R.H. 1971: Remote sensing of ocean currents and sea surface temperature changes derived from the Nimbus II satellite. J. Phys. Oceanog., 1(1), 45-60.

Occasional Papers

INSTITUTE OF ARCTIC AND ALPINE RESEARCH

Occasional Paper No. 1: The Taxir Primer, R.C. Brill, 1971.

Occasional Paper No. 2: Present and Paleo-Climatic Influences on the Glacierization and Deglacierization of Cumberland Peninsula, Baffin Island, J. T. Andrews and R. G. Barry, and others, 1972.

Occasional Paper No. 3: Climatic Environment of the East Slope of the Colorado Front Range, R. G. Barry, 1972.

Occasional Paper No. 4: Short-Term Air-Sea Interactions and Surface Effects in the Baffin Bay - Davis Strait Region from Satellite Observations, J.D. Jacobs, R.G. Barry, B. Stankov and J. Williams, 1972.